



MARMARA UNIVERSITY  
FACULTY OF MECHANICAL  
ENGINEERING



## Modeling of Pressure Drop Methodology in Refrigeration Cycles and its Implementation

Habip Akin HACIMUSALAR

Müdekkilik Final Project Commission			
The essential features of an acceptable design Project			
	Satisfied	Unsatisfied	
1 Mechanical or Thermal Design	✓		
2 Report writing technique	✓		
3 Development of student creativity		✓	
4 Use of open-ended problems		✓	
5 Formation of design	✓		
6 Problem statement and specification	✓		
7 Synthesis of alternative solutions		✓	
8 Feasibility	✓		
9 Detailed system description	✓		
10 Consideration of constraints (e.g. economic, safety, reliability, etc.)		✓	
11 Utilization of engineering and scientific principle	✓		
Decision	Signature		
Accepted but not approved	17.07.2021		
Prof. Dr. Bülent Ekici,			
Dr. Öğr. Üyesi Uğur Tümerdem			
Ar. Gör Serkan Öğüt			

## GRADUATION PROJECT REPORT Department Of Mechanical Engineering

Supervisor

Asst. Prof. Mehmed Rafet OZDEMIR

ISTANBUL, 2021



**MARMARA UNIVERSITY  
FACULTY OF MECHANICAL  
ENGINEERING**



**Modeling of Pressure Drop Methodology in Refrigeration Cycles and  
its Software Implementation**  
by

**Habip Akin HACIMUSALAR**

**July, 2021, Istanbul**

**SUBMITTED TO THE DEPARTMENT OF MECHANICAL ENGINEERING  
IN PARTIAL FULFILLMENT OF THE REQUIREMENTS FOR THE  
DEGREE**

**OF  
BACHELOR OF SCIENCE  
AT MARMARA UNIVERSITY**

**The author hereby grants to Marmara University permission to reproduce and to  
distribute publicly paper and electronic copies of this document in whole or in  
part and declare that the prepared document does not in any way include  
copying of previous work on the subject or the use of ideas, concepts, words, or  
structures regarding the subject without appropriate acknowledgement of the  
source material.**

Signature of Author

Habip Akin Hacimusalar

Certified By ..... Department of Mechanical Engineering  
.....Asst Prof..Dr..Mehmed.Rafet.Özdemir

Accepted By ..... Project Supervisor, Department of Mechanical Engineering  
.....Prof.Dr.Bülent.EKİCİ  
Head of the Department of Mechanical Engineering

## **ACKNOWLEDGEMENT**

This report represents the end of my undergraduate life at Marmara University Engineering Faculty Mechanical Engineering Department and the beginning of my engineering life. This report and the preparation process have contributed me to understand the basics and the soft skills of mechanical engineering and my future life. I would like to show my appreciation to those who helped me to complete my first and hopefully many achievements in this area.

First of all, I would like to thank my supervisor Asst. Prof. Dr. Mehmed Rafet ÖZDEMİR, who encouraged me constantly and shared his experience with me. I also thank Mr. Özdemir for leading me through the finishing project and lighting my path with his in-school and out-school experience and guidance and appreciate his in-depth knowledge.

I would like to thank FRITERM Inc. R&D Engineer Mehmet Harun SÖKÜCÜ, who provided me all kinds of support during the project work, day-in and day-out. I would like to thank him due to his vast patience ahead of my persistent questions and his vast support.

I would like to thank every single lecturer that I had chance to be a participant of their classes.

Most important and final, I am grateful to my mother, father, and brother for their support during my seventeen years of education and their guidance on me.

**Habip Akin HACIMUSALAR**

**July, 2021-ISTANBUL**

## TABLE OF CONTENTS

ACKNOWLEDGEMENT .....	i
ABSTRACT .....	iv
ABBREVIATIONS & SYMBOLS .....	v
LIST OF FIGURES .....	vi
LIST OF TABLES .....	ix
1. INTRODUCTION .....	1
2. REFRIGERATION CYCLES .....	4
2.1 Mechanical Vapor Compression Cycle .....	4
2.2 Refrigeration Cycle Elements.....	7
2.2.1 Compressor.....	7
2.2.2 Condenser .....	7
2.2.3 Expansion Valve.....	8
2.2.4 Evaporator .....	8
2.3 P-h & T-s Diagrams on Refrigeration Cycle and Super-Heating & Sub-Cooling .	9
2.3.1 Super-Heating.....	9
2.3.2 Sub-Cooling.....	9
2.3.3 Comparison of Theoretical and Actual Refrigeration Cycle .....	10
3. REFRIGERANT DISTRIBUTOR .....	12
4. TWO PHASE FLOW .....	15
4.1 Two Phase Pressure Drop Methodology .....	15
4.1.1 Theoretical Background on Two-Phase Pressure Drop Calculations.....	17
4.1.2 Dimensionless Number of Fluid Flow .....	22
4.2 Flow Regime Maps in Horizontal Tubes.....	24
4.3 Two-Phase Pressure Drop Models .....	30
4.3.1 Analytical Methods .....	31
4.3.2 Phenomenological Methods .....	31
4.3.3 Empirical Methods .....	32
4.4 Nozzle Pressure Drop .....	37
5. EXPERIMENTEL SETUP .....	39
5.1 Laboratory Explanation .....	39
5.2 Electronic Control Principles.....	42
5.3 Experiment Sample .....	45

5.4 Theoretical Validation Setup: Commercial Software.....	46
6. Developed Two Phase Pressure Drop Software .....	49
6.1 Refrigerant Property Integration.....	49
6.2 Interface Creation .....	50
6.3 Implemented Codes on Interface .....	53
6.3.1 Upper Body and Code Transformation between Run Buttons .....	53
6.3.2 Lower Body Correlation Implementation.....	56
7. RESULT and DISCUSSION.....	64
7.1 Existing Software and Developed Software Comparisons.....	64
7.2 Experimental Data and Developed Software Comparison .....	70
7.3 Discussion.....	76
8. CONCLUSION & RECOMMENDATION.....	78
9. BIBLIOGRAPHY .....	79
10. APPENDIX .....	82

## ABSTRACT

In refrigeration cycles, evaporators are used to cool the ambient so thus evaporating the refrigerant they have by absorbing heat from the air passes through evaporator coils. During this process external devices such as, thermal expansion valve, condenser, compressor, distributor are used. These devices play crucial role on refrigeration process. The path that the refrigerant followed after thermal expansion valve is very important for us. After thermal expansion valve, refrigerant reach its two-phase and it is aimed to distribute this refrigerant homogenously on evaporator tubes. For this purpose, distributors are used.

Calculating the suitable distributor and tube diameter, are very important to distribute the refrigerant homogenously. For this purpose, we always seek to find most accurate pressure drop during this process. This thesis is studied to develop a software to find pressure drop on both nozzle and evaporator coils. Because, by knowing how much pressure change occurs in the system, we can eliminate inhomogeneous fluid flow to evaporator tubes and we can increase the efficiency of the system.

Although, there are existing products in the industry for this purpose, these products may not give accurate results and they may not consider important features. This study is aimed to developed new software for determining the pressure drop and adding new features so increasing the accuracy of founding pressure drop.

The developed software, yields the output for most cases within 15% of accuracy. This study is validated by experimental reports that conducted with the investigation of FRITERM Inc. and their test laboratory.

**Keywords:** Refrigeration Systems, Evaporator, Pressure Drop, Two-Phase Flow-Software Development

## ABBREVIATIONS & SYMBOLS

$P$	Pressure (kPa)	$\epsilon$	Void Fraction
$\dot{x}$	Vapor Quality	$G$	Mass Flux $\left(\frac{kg}{m^2 s}\right)$
$\rho$	Density ( $kg/m^3$ )	$V$	Velocity $\left(\frac{m}{s}\right)$
$h$	Enthalpy (kj/kg)	Re	Reynolds Number
$T$	Temperature ( $^\circ C$ )	Nu	Nusselt Number
$C_p$	Heat Capacity at Constant Pressure (kj K/kg)	Fr	Froude Number
$C_v$	Heat Capacity at Constant Volume (kj K/kg)	Pr	Prandtl Number
$P_{crit}$	Critical Pressure (kPa)	$X_{tt}^2$	Martinelli Parameter on Regime Map
$P_{sat}$	Saturation Pressure (kPa)	T	Regime Map Parameter
$T_{crit}$	Critical Temperature ( $^\circ C$ )	K	Regime Map Parameter
$T_{sat}$	Saturation Temperature ( $^\circ C$ )	$\Phi_l^2$	Martinelli Parameter on liquid
$\Delta P_{total}$	Total Pressure Drop (kPa)	$\Phi_g^2$	Martinelli Parameter on Gas
$\Delta P_{acc}$	Acceleration Pressure Drop (kPa)	f	Friction Factor
$\Delta P_f$	Frictional Pressure Drop (kPa)	$\Phi_{Ch}^2$	Chisholm two-phase Multiplier
$\Delta P_N$	Nozzle Pressure Drop (kPa)	B	Chisholm Parameter
$\dot{M}$	Mass Flow Rate $\left(\frac{kg}{s}\right)$	$\beta$	Nozzle Diameter and Pipe Diameter Ratio
$C_d$	Nozzle Coefficient		

## LIST OF FIGURES

Figure 1 Refrigeration Cycle Schematic .....	1
Figure 2 Simple Vapor Compression Refrigerant Cycle [6] .....	5
Figure 3 Processes are represented on a P-h and T-s chart as shown in fig. (a) and (b) respectively. [6] .....	6
Figure 4 Condenser Coils [7] .....	7
Figure 5 Expansion Valve [8].....	8
Figure 6 Evaporator Coil [7] .....	8
Figure 7 Refrigeration Cycle Schematic [9].....	9
Figure 8 Comparison of Reversed Rankin and Carnot Cycle [9].....	10
Figure 9 T-s Diagram [9].....	11
Figure 10 P-H Diagram [9].....	11
Figure 11 TEV & Distributor Schematic [10] .....	12
Figure 12 Homogenous & Non Homogenous Representation of Refrigerant [10].....	13
Figure 13 Distributor Evaporator Tube Connections [10] .....	13
Figure 14 Distributor Types .....	14
Figure 15 Friterm A.S Distributor Models on Front View.....	14
Figure 16 Friterm A.S Distributor Models on Top View .....	14
Figure 17 Two-Phase Flow Classification.....	17
Figure 18 Cross-Sectional Void Fraction .....	19
Figure 19 Values for $C_o$ and $u_{gi}$ [14].....	20
Figure 20 a) Stratified Flow b) and c) Stratified Bubble Flow [15] .....	25
Figure 21 Intermittent Flow Regime a) 9.52 mm Tube b) and c) 15.8 mm tube [15]....	25
Figure 22 Annular Flow Regime a) 9.52 mm Tube b) and c) 15.8 mm tube [15] .....	26
Figure 23 Regime Map that belongs to Taitel and Dukler (1976).....	26
Figure 24 a) Taitel and Dukler Two-phase flow pattern map b) asymmetric liquid film profiles c) Cioncolini and Thome updated version of regime map [15] .....	27
Figure 25 Updated Version of Taitel & Dukler and its software implementation basis	28
Figure 26 Study of Collier and Thome (1994) existing flow patterns during evaporation .....	29
Figure 27 Schematic Representation of the Experiment Setup. LHS Air-Conditioning Chamber and RHS Calorimetric Chamber .....	40

Figure 28 a) Air-Conditioning Chamber b.) Calorimetric Chamber .....	40
Figure 29 Schematic Representation of Water Line.....	41
Figure 30 Superheat Control Scheme .....	41
Figure 31 Measurement System Schematic.....	42
Figure 32 Agilent 34970A datalogger and Yokogawa WT210 Digital Power Measurement Device .....	43
Figure 33 PID Scheme of the Experimental Setup.....	44
Figure 34 Experiment Sample that Provided by Friterm.....	45
Figure 35 Commercial Software.....	46
Figure 36 Commercial Software Interface .....	47
Figure 37 Output Interface of the Existing Software .....	48
Figure 38 Software Interface .....	50
Figure 39 Upper Body of the Interface.....	51
Figure 40 Lower Body of the Interface .....	51
Figure 41 Property Callback Codes .....	53
Figure 42 Refrigerant Data Conduction Codes .....	54
Figure 43 Mass Flow Rate Calculation Codes .....	54
Figure 44 Refrigerant Property Codes.....	55
Figure 45 Diameter Elimination Codes .....	55
Figure 46 Answer Representation Codes .....	56
Figure 47 Error Determination and End of 1 <sup>st</sup> Run Button .....	56
Figure 48 2 <sup>nd</sup> Run Button Input Reading.....	56
Figure 49 Nozzle Orifice Number Reading Loop .....	57
Figure 50 Pipe Size Reading Loop .....	57
Figure 51 Necessary Equations, Area and Mass Flux Calculation.....	58
Figure 52 Void Calculations.....	58
Figure 53 Necessary Equations .....	59
Figure 54 Regime Map Primary Foundings .....	59
Figure 55 Regime Map Secondary Foundings .....	60
Figure 56 Regime Map Boundary Codes .....	60
Figure 57 Regime Map Friction Factor Codes .....	60
Figure 58 Nozzle Pressure Drop Codes.....	61

Figure 59 Acceleration Pressure Drop Codes .....	61
Figure 60 Frictional Pressure Drop Codes .....	61
Figure 61 Percent Loading reading and Iteration .....	62
Figure 62 Last Coding lines.....	63
Figure 63 Case 7.1.1 Existing Software .....	64
Figure 64 Case 7.1.1 Developed Software .....	64
Figure 65 Case 7.1.2 Existing Software .....	65
Figure 66 Case 7.1.2 Developed Software .....	65
Figure 67 Case 7.1.3 Existing Software .....	66
Figure 68 Case 7.1.3 Developed Software .....	66
Figure 69 Case 7.1.4 Existing Software .....	67
Figure 70 Case 7.1.4 Developed Software .....	67
Figure 71 Case 7.1.5 Existing Software .....	68
Figure 72 Case 7.1.5 Developed Software .....	68
Figure 73 Case 7.2.1 Developed Software Output.....	70
Figure 74 Case-7.2.2 Developed Software Output.....	71
Figure 75 Case-7.2.3 Developed Software Output.....	72
Figure 76 Case-7.2.4 Developed Software Output.....	73
Figure 77 Case-7.2.5 Developed Software Output.....	74

## **LIST OF TABLES**

Table 1 C value that fits into Lockhart and Martinelli Equation.....	34
Table 2 Cd Coefficient Table .....	38
Table 3 Properties of Measurement Devices.....	42
Table 4 Comparison of Existing Software vs Developed Software .....	69
Table 5 Existing Software and Developed Software Output Accuracy Analysis .....	69
Table 6 Experimental Case-7.2.1 .....	70
Table 7 Experimental Case-7.2.2 .....	71
Table 8 Experimental Case-7.2.3 .....	72
Table 9 Experimental Case-7.2.4 .....	73
Table 10 Experimental Case-7.2.5 .....	74
Table 11 Comparison of Experimental Data and Software Output.....	75
Table 12 Experimental Data and Software Output Accuracy Analysis .....	75

## 1. INTRODUCTION

The refrigeration cycle is a critical component of HVAC systems and is governed by the principles of thermodynamics. It plays a crucial role in our daily life. We encounter different types of refrigeration usage from commercial food management to daily home and/or office routines.

Refrigeration cycle operates with the principle of the transfer of heat from a lower temperature region to a higher temperature one[1]. A standard refrigerator works as the various combination of mechanical elements that make it easy for it to achieve and maintain desired temperatures. There are different components that help refrigeration cycle to maintain its purpose. These components are highly specialized in order to provide desired effects. There are four main components that vapor compression cycle has. These components are:

- Evaporator
- Compressor
- Expansion Valve
- Condenser

In Figure 1 basic representation of a refrigeration cycle is given.

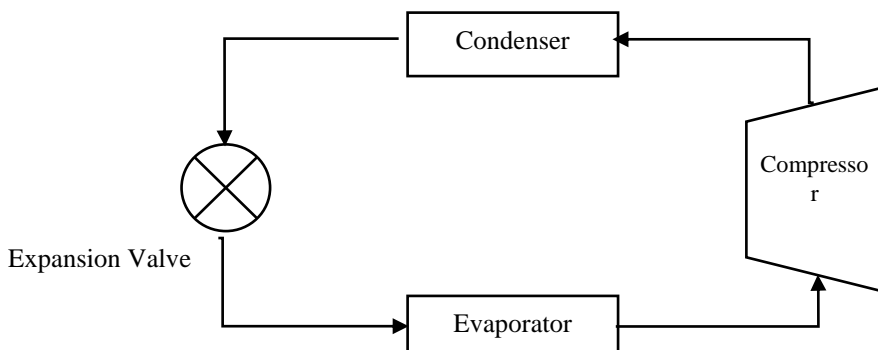


**Figure 1** Refrigeration Cycle Schematic

While each of the components- that are counted above- have their specialized sub-components, we will be dealing with distributor which takes part right after expansion valve and before evaporator.

While some refrigeration cycles work with one phase refrigerant, some are required to use two phase refrigerants. In this two-phase flow, we will be dealing with liquid-vapor mixture. The distributor is used to satisfy distribution of these two phases into homogenous flow to each evaporation tube so thus increasing the COP of the cycle and keeping the pressure drop at the appropriate values. The way to increase COP is to satisfy homogenous flow distribution as much as possible. By the light of experimental studies, it is stated that COP plays role between 10-15% efficiency in the refrigeration cycle design[2]. Also, having the knowledge of theoretical pressure drop prior to experimental setup, gives us chance to re-consider distributor selection so thus controlling the cycle in more effective and convenient way.

Theoretical estimation of pressure drop in refrigeration cycle and its homogenous distribution is not an easy issue to dealt with. Gravity, heat transfer, pressure drop, selected refrigerant, placement of refrigeration system are very influential on the distribution in the distributor. Too many researches are done to estimate single phase pressure drop and it analyzes become less confusing and more accurate. However, the same situation is not valid for two phase pressure drop. With the studies start from middle of 20<sup>th</sup> century, too many applications and correlations are developed and the studies proved that two-phase flow analysis are highly relied on mass quality ( $\dot{x}$ ) of the refrigerant[3].

The reason why it is aimed to distribute refrigerant into evaporator tubes is to increase efficiency of the cycle. To demonstrate, non-homogenous fluid flow in the evaporator cause hunting (non-continues refrigerant flow from expansion valve due to high pressure drop) in the expansion valve, refrigerant mixture on the compressor (due to being not able to absorb sufficient heat and less evaporation), and oil accumulation in the evaporator due to insufficient feedback.

Throughout the years, so many studies are held on pressure drop estimation on two phase flow. Different methodologies occurred with their own correlations. Different pressure drop softwares are developed to analyze this phenomenon and find accurate theoretical calculations.

Since these commercial softwares use relatively old correlations, and not consider some important features -such as flow regime, superheating & subcooling- sometimes they may not yield to accurate pressure drop result. Due to this issue, developing new softwares that calculate pressure drop in a more accurate and convenient way is aimed to study.

In this thesis study, examination of two-phase pressure drop will be covered and pressure drop methodology will be developed as brand-new software. With software, accuracy of theoretical calculations will be increased and consistent distributor selections will be able to operate.

## **2. REFRIGERATION CYCLES**

Refrigeration can be stated as heat absorption from the body and/or cooling it. The idea is forcing the ambient state to become cooler than the previous state. To cool a space or body, heat should be absorbed from it and extracted to outer space. The mechanic system that makes this process is called refrigeration cycle. In that sort of special processes, not just heat absorbing but,

- Safety conditions must be satisfied and sustainable solutions should be aimed,
- Body or the ambient should reach the target heat in specified time and or conditions,
- The physical properties of the body should be affected as low as possible,
- Least energy should be consumed and Coefficient of Performance (COP) should be as high as possible,

There are four different types of refrigeration cycles. These types are:

- Mechanical Vapor Compression Refrigeration Cycle
- Absorption Cycle
- Evaporative Cooling
- Thermoelectric Refrigeration

Instead of these four, specialized refrigeration cycles are also existing. Mechanical compression refrigeration cycle is known as the most common type in usage. Since its vast area of usage and serving the methodology that we created, I would like to cover mechanical compression refrigeration cycle briefly than move forward.

### **2.1 Mechanical Vapor Compression Cycle**

The most frequently used cycle for refrigeration is vapor-compression refrigeration cycle and it involves four main components: an evaporator, a compressor, an expansion valve, and a condenser. [4]

At the beginning of the cycle, single-phase or two-phase refrigerant meets the compressor as vapor of low temperature vapor and low pressure. Compressor increases the pressure and temperature of the refrigerant and the refrigerant becomes superheated gas. High temperature and high-pressure gas then pass through the condenser that it releases heat to the surroundings as it cools down and complete its condensation. After condenser, high pressure liquid moves to thermal expansion valve to reduce its pressure and become two-phase cooler refrigerant. This mixture mostly contains liquid and vapor only and by hitting the distributor, refrigerant moves into evaporator where it vaporizes completely as it absorbs heat from the surroundings prior to returning to the compressor as low temperature and low pressure gas to start the cycle again. [5]

In Fig. 2 vapor compression cycle schematic is given.

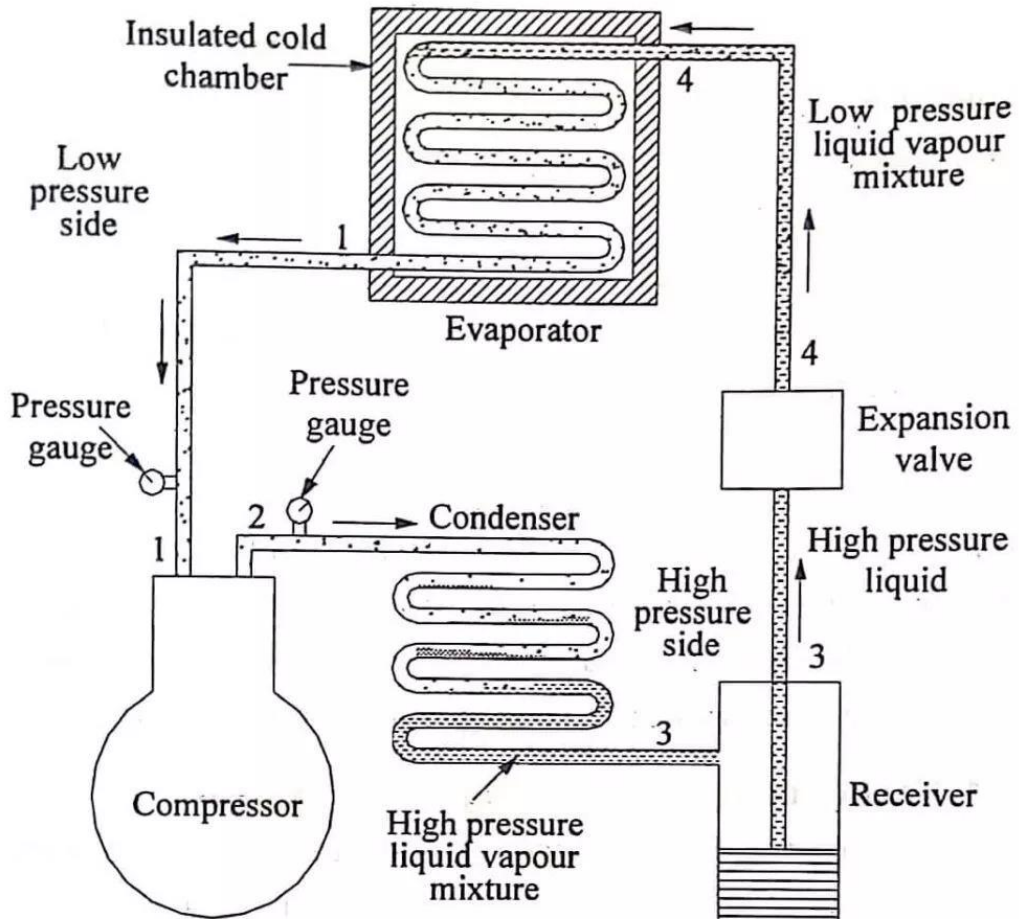


**Figure 2** Simple Vapor Compression Refrigerant Cycle [6]

The high pressure vapor refrigerant that exits from the condenser is follow the path through the expansion or throttle valve that it expands to required pressure. The pressure is reduced throughout expansion, and the vapor is partially converted to liquid, resulting in a cooling effect. This process is represented in p-h diagram as 3-4.

The expansion valve sends a mixture of low-temperature vapor and liquid into the evaporator, which absorbs heat from the refrigerated environment. This process is represented in p-h diagram as 4-1.

After evaporation, two-phase liquid vapor becomes vapor (state 1) and this vapor enters the compressor. It is compressed there, and as its result, pressure rises. This process is represented in p-h diagram as 1-2.

This high-pressure vapor enters the condenser. There, it loses its latent heat and becomes liquid. This process is represented in p-h diagram as 2-3. The cycles follow this loop and it keeps on working.

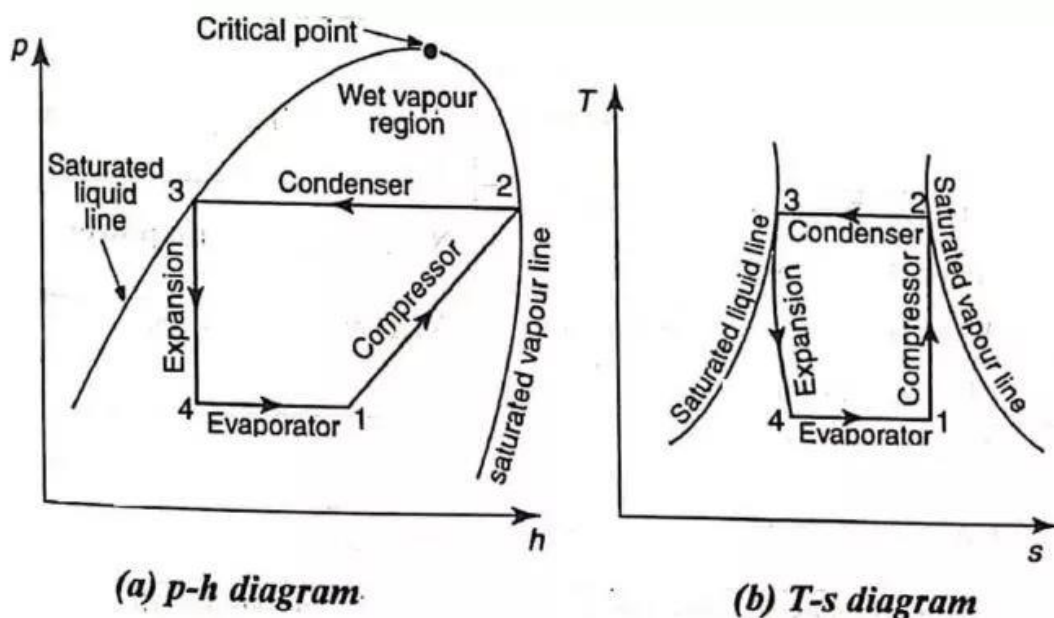


**Figure 3** Processes are represented on a P-h and T-s chart as shown in fig. (a) and (b) respectively. [6]

## 2.2 Refrigeration Cycle Elements

Mechanical Vapor Compression Cycles is a combination of four-cycle elements. These elements are:

- Compressor
- Condenser
- Expansion Valve
- Evaporator

### 2.2.1 Compressor

The first phase in the refrigeration cycle is compression that raises the operating refrigerant's pressure. Low-pressure, low-temperature refrigerant enters compression as a low-pressure, low-temperature gas and exits as a high-pressure, high-temperature gas.

### 2.2.2 Condenser

In a basic refrigeration loop, the condenser is one of two types of heat exchangers. This component receives vaporized refrigerant from a compressor that is high-temperature and high-pressure. The condenser extracts heat from the heated refrigerant gas vapor until it condenses into a saturated liquid condition. After condensing, the refrigerant contains high-pressure, low-temperature liquid, and moves into expansion valve.



**Figure 4** Condenser Coils [7]

### **2.2.3 Expansion Valve**

These parts are available in a variety of styles. Fixed orifices, thermostatic expansion valves or thermal expansion valves, and advanced valves are all popular types. The expansion device, regardless of configuration, causes a pressure decrease after the refrigerant leaves the condenser. Because of the pressure reduction, some of the refrigerant will boil quickly, resulting in a two-phase mixture. This rapid phase change is known as flashing, and it assists the evaporator, the next piece of equipment in the cycle, in performing its job adequately. From expansion valve, refrigerant hit the distributor and its homogenous distribution to evaporator is aimed.



**Figure 5** Expansion Valve [8]

### **2.2.4 Evaporator**

In the refrigeration cycle, the evaporator is the second heat exchanger that follows the loop. The evaporator receives low-temperature refrigerant, which absorbs heat from the refrigerated compartment and evaporates. Once the refrigerant exits the evaporator and returns to the compressor, the cycle is complete. Pressure drop occurs in this section as well and we are highly interested in it. Developed software is also aimed to determine pressure drop in single evaporator coil.

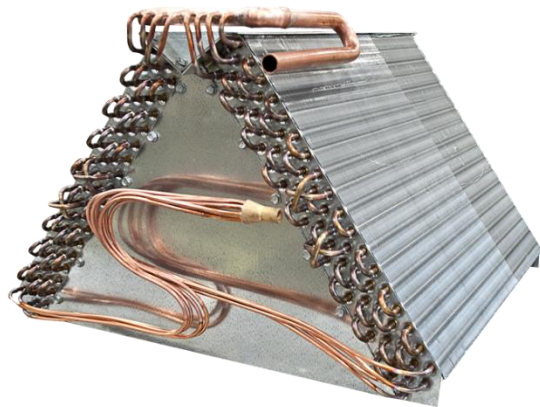


**Figure 6** Evaporator Coil [7]

## 2.3 P-h & T-s Diagrams on Refrigeration Cycle and Super-Heating & Sub-Cooling

The refrigeration systems are based on satisfying the second law of thermodynamics. The process will be explained briefly with the help of the schematic diagram in **Fig 7**. While talking about the theoretical and actual refrigeration cycle, we will mention refrigerant cycle as reversed Carnot Cycle. Before proceeding the working principle of the refrigeration cycles, let's take a look at subcooling and super-heating.

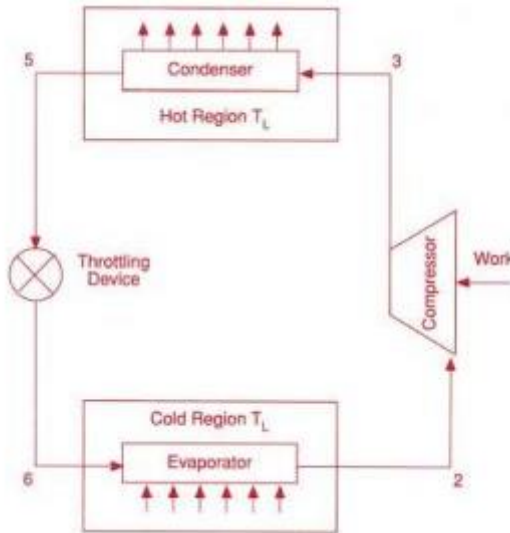


**Figure 7** Refrigeration Cycle Schematic [9]

### 2.3.1 Super-Heating

Refrigerant follow a curved line on their p-h diagram. In the boundary of this curve, two phase is existing. If the location of the refrigerant on p-h diagram is exceeded the boiling point, superheating is occurred. This process will be examined under P-h diagram in a better form.

### 2.3.2 Sub-Cooling

At the compressor exit pressure, the refrigerant is assumed to leave the condenser as a saturated liquid. In reality, some pressure drop in the condenser, as well as the lines connecting the condenser to the compressor and the throttling valve, is unavoidable. Furthermore, it is difficult to carry out the condensation process to the point where the refrigerant is a saturated liquid at the conclusion, and it is undesirable to direct the refrigerant to the throttling valve before it is totally condensed. As a result, the refrigerant is slightly cooled before entering the throttling valve. [1]

### 2.3.3 Comparison of Theoretical and Actual Refrigeration Cycle

The real-world vapor compression cycle is not the same as the theoretical vapor compression cycle. Condensation and evaporation do not occur at constant pressure in a real-world cycle. Also, compression is not isentropic and the overall Coefficient of Performance of the actual cycle is lower than the theoretical cycle. Refrigeration cycle - Reversed Carnot Cycle - doesn't work in practical cases. In practice, the reversed Carnot Cycle does not function. Two isentropic and isotherm processes make up the reversed Carnot Cycle. When theoretical Carnot cycle is completely reversible, this is not valid for reversed Rankine cycle due to losses in the condensers, evaporators, and compressors. As a result, a more practical and realistic Rankin cycle with two isobaric processes, one isentropic compression, and one adiabatic expansion has been developed. Let us examine theoretical and real diagrams via considering physical limitations and subcooling superheating.

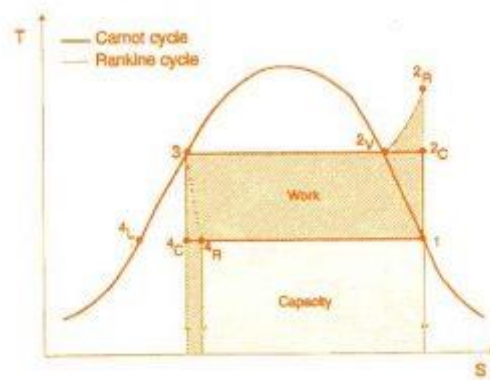


**Figure 8** Comparison of Reversed Rankin and Carnot Cycle [9]

Isentropic compression and isothermal heat absorption and rejection are two totally reversible processes that can never be achieved in a cycle. However, other processes, like as subcooling and superheating, actually aid in the proper operation of refrigerator components. When comparing the ideal/theoretical vapor compression cycle to the actual vapor compression cycle, it is clear that assuming the ideal refrigeration cycle will simplify computations.

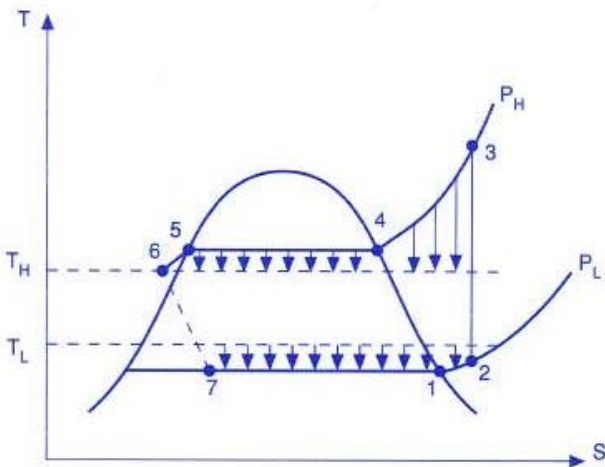


**Figure 9** T-s Diagram [9]

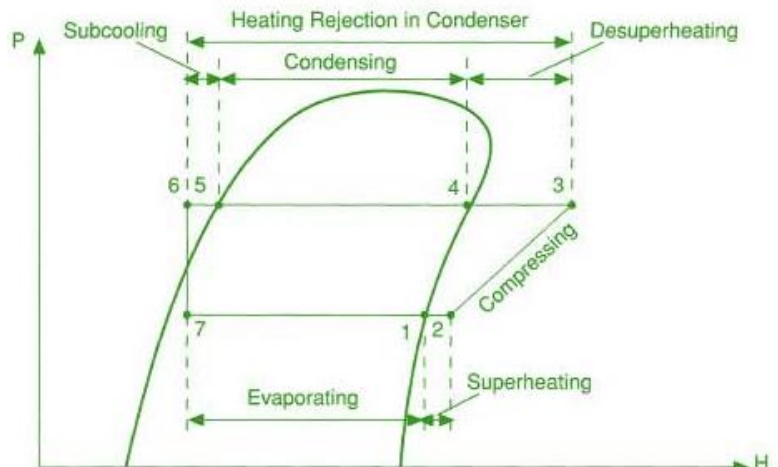


**Figure 10** P-H Diagram [9]

The cycle follows the steps that given below [9]:

- 7-1: Evaporation of the liquefied refrigerant (coming from the condenser) taking place at a constant temperature. The process is isothermal. ( $T_1 = T_7$ )
- 1-2: The vapor coming from the evaporator is superheated and gains the temperature  $T_2$  from  $T_1$  at constant pressure  $P_L$ . The process is isobaric.
- 2-3 The superheated working fluid is compressed. Pressure rises from  $P_L$  to  $P_H$
- And the temperature rises from  $T_2$  to  $T_3$
- 3-4 The superheated vapor is cooled to the saturated temp  $T_3$ .
- 4-5 Isothermal condensation of the saturated vapor at high-pressure  $P_H$ . and  $T_4=T_5$
- 5-6 The liquid refrigerant is subcooled to the temperature  $T_6$  from  $T_5$  at high-pressure  $P_H$ .
- 6-7 The expansion of the refrigerant takes place at constant enthalpy.

### 3. REFRIGERANT DISTRIBUTOR

A refrigerant distributor is a device that connects to the outlet of a thermostatic expansion valve (TEV) to evenly distribute refrigerant flow from the TEV into each circuit of a multi-circuit evaporator coil. The distributor's outlet has been modified to accept tubing that links it to each evaporator coil circuit. Thermal Expansion Valve and distributor tube connections are represented in **Fig.11**.

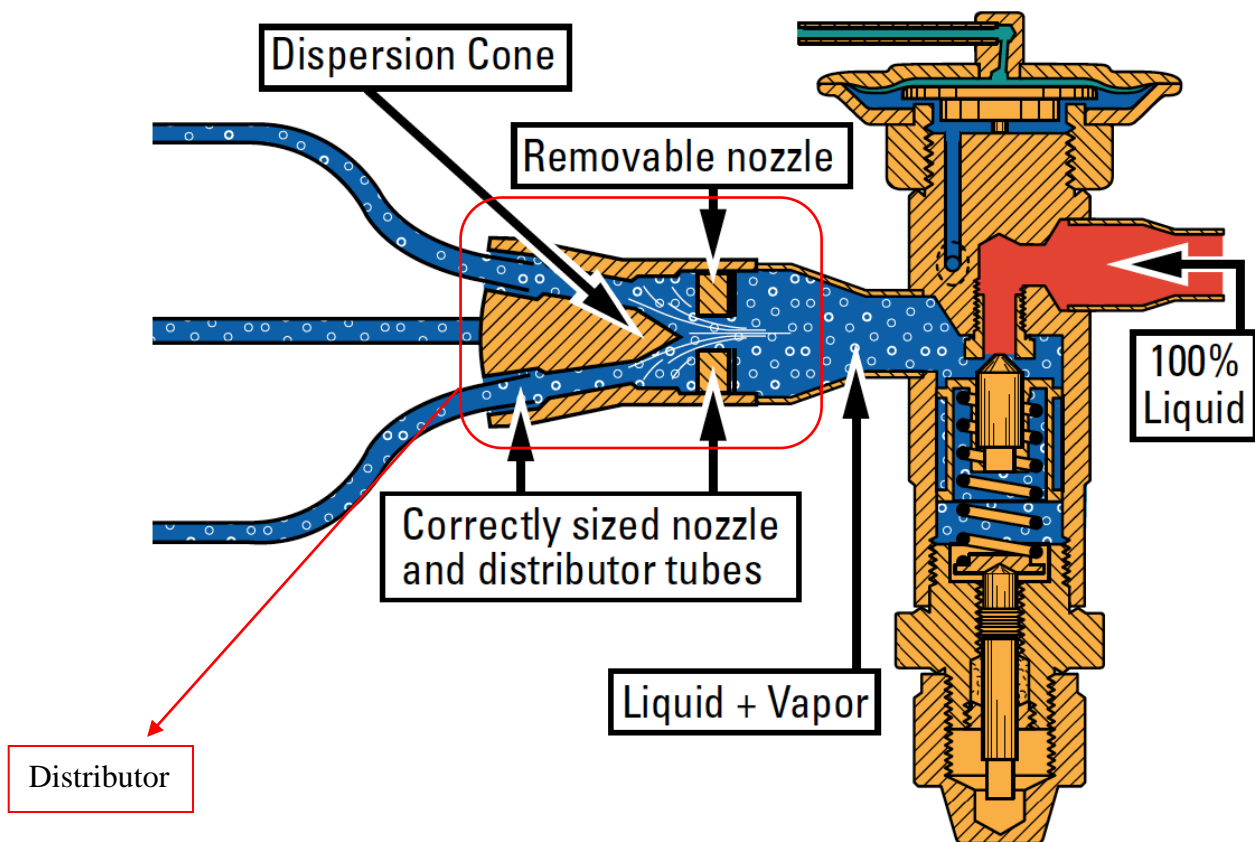


**Figure 11** TEV & Distributor Schematic [10]

Since refrigerant distribution has a direct impact on the operation of the thermostatic expansion valve and the evaporator coil, it is critical for proper system performance. If refrigerant cannot be distributed homogeneously through the evaporator coil, the thermostatic expansion valve will often hunt and may result in occasional flood back to the compressor. Since this circuits in the coil aren't fully active, the evaporator's performance will decrease as well.

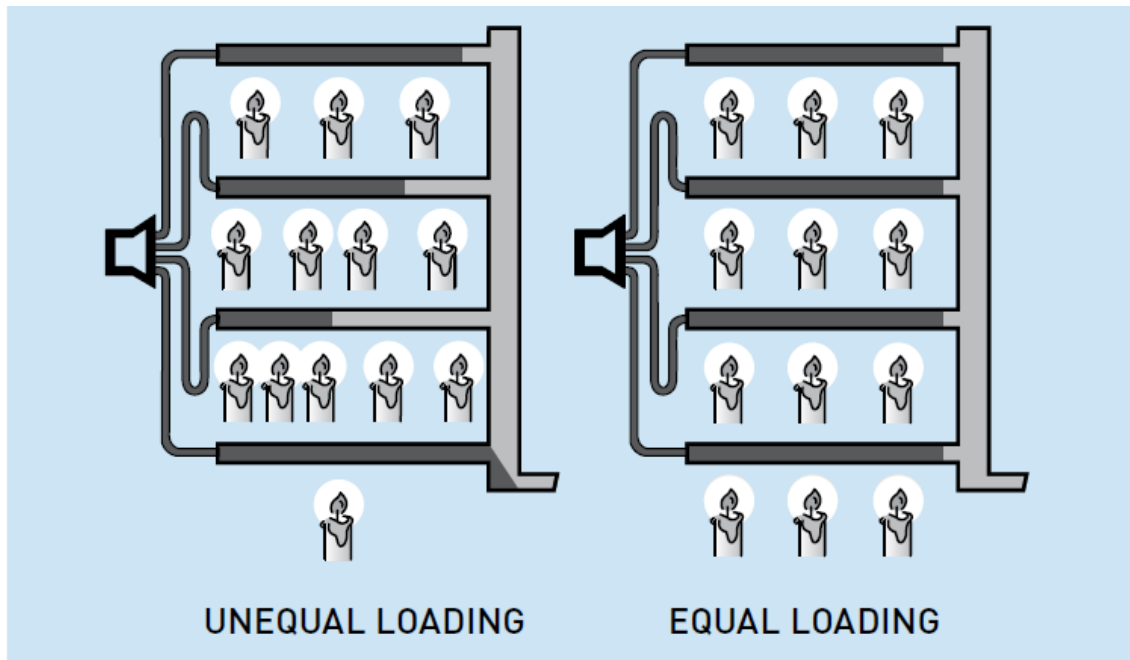


**Figure 12** Homogenous & Non Homogenous Representation of Refrigerant [10]

Different types of distributors and their mounting types are existing. The mounting can be;

- Up Feed
- Down Feed
- Side Feed

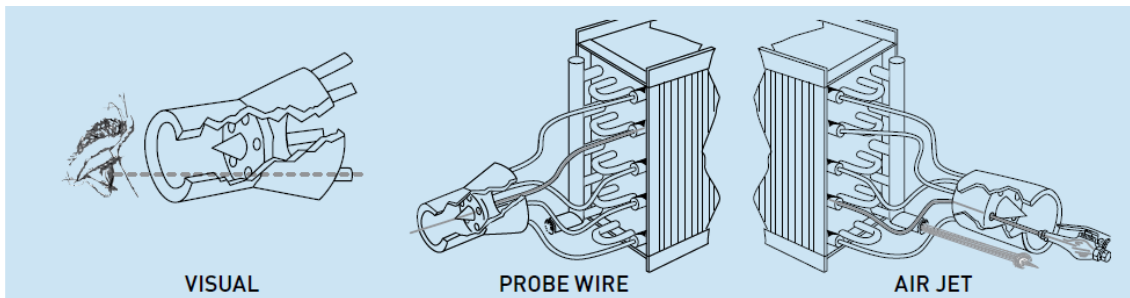
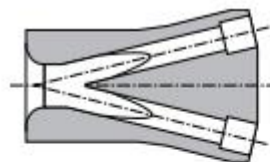


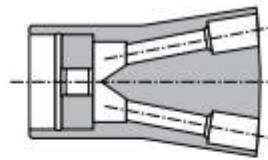
**Figure 13** Distributor Evaporator Tube Connections [10]

There are two types of distributor type and selection criteria. These types are:

- Venturi Type Distributor
- Nozzle Distributor



**Venturi Distributor**



**Nozzle Type Distributor**



**Figure 14** Distributor Types

In figure 15 and 16, three different types of Distributors with different nozzle orifice number, length and circuit number are given.

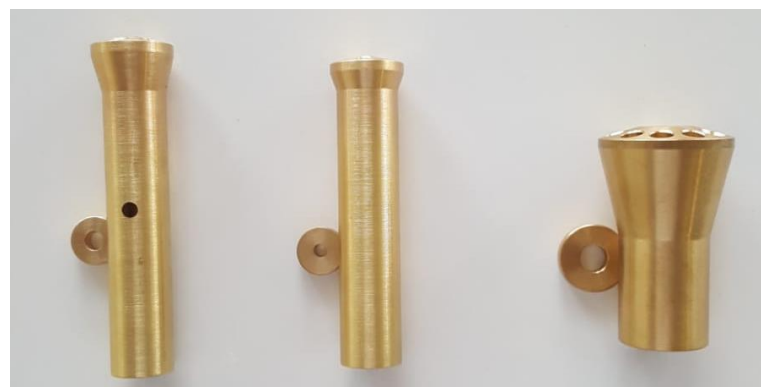


**Figure 15** Friterm A.S Distributor Models on Front View



**Figure 16** Friterm A.S Distributor Models on Top View

## **4. TWO PHASE FLOW**

A two-phase flow occurs when two different aggregation states of a substance or two different substances are present at the same time. The possible combinations of two-phase flow are:

- gaseous/liquid
- gaseous/solid
- liquid/solid.

Two phase flow, is commonly encountered in major scaled power units. These types of flow have high usage in the industry. To demonstrate, coal and gas fired power cycles refers to steam-liquid mixes, usage of gas-liquid flow in evaporator and condenser during evaporation and condensation, gas-liquid-solid flow in chemical reactors, two immiscible liquids that does not mix during oil recovery process.

In this section, two phase flow pressure drop methodology and its regime map will be discussed. Properties and characteristics of two-phase flow will be examined for liquid/gas.

### **4.1 Two Phase Pressure Drop Methodology**

Throughout out the years, so many studies are developed on single phase pressure drop methodology. While some of these methodologies are still in use, some of them lead new developments and leave their places on latest accurate studies.

While making accurate prediction is quite possible on single phase flow, two phase flow has its own obstacles. These obstacles are coming from special characteristics of two phase and analytical difficulty on this area.

The obstacles of two-phase flow prediction come from:

- High Density difference in two phase flow. This difference effects the pressure drop, and effect of flow regimes onto heat transfer and phase ratio
- Viscosity difference also cause the similar problem that is counted above
- The change of the velocity of the fluids undergoing phase change in the channel and the characteristic of the flow changes, so that analytical analysis is made onto compressible fluid characteristics
- Expressing heat transfer and pressure drop with different correlations and difficulties on calculating the exact pressure drop
- As the analytical solutions are complicated and the groping solution is quite difficult to proceed

To overcome the difficulties on pressure drop calculation, some approaches are made and single phase based correlations are developed. These approaches are:

- Experimental methodology development that based on real life scaled laboratory models
- Theoretical calculations by using mathematical models and equations
- Numerical analysis by using high capability of modern computers

While real life scaled laboratory model setup is applicable in some applications, some does not allow this because prototype needs to have different sizes. Prior to experimental setup, theoretical and numerical calculations must be done to ensure the safety of the experiment. These numerical and theoretical calculations play crucial role on the cases which is hard to model due to its cost, technical differences etc.

Classification of internal flow is also made with respect to tube replacement- horizontal or vertical-. In horizontal flow, gravity effects seen on the refrigerant and that cause liquid phase of the mixture to fall down therefore gas accumulates on the higher part of the tube.

In vertical flow, 2 phase refrigerant makes its move on upwards and downwards. Gravity effect on the tube expressed as symmetric on the flow axis.

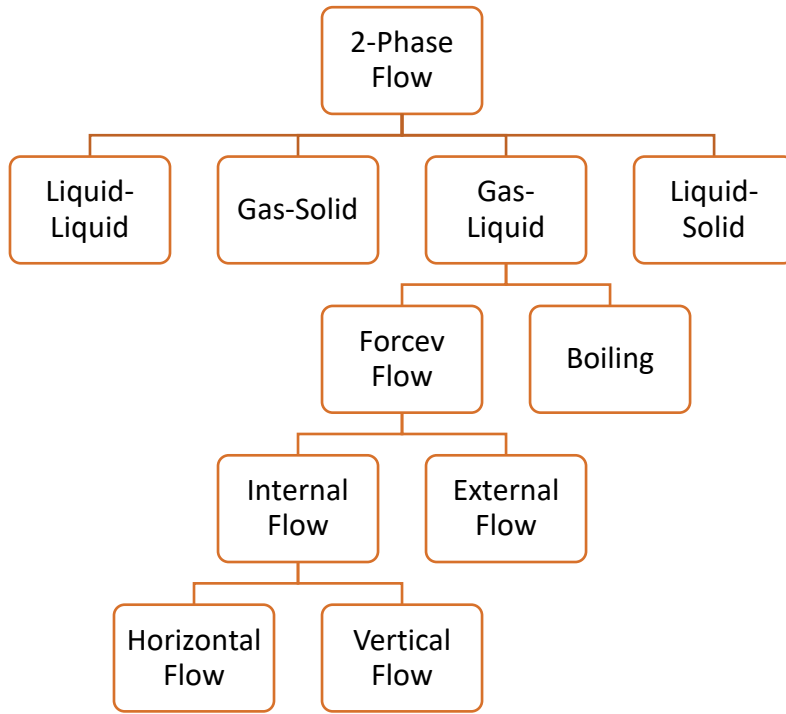


**Figure 17** Two-Phase Flow Classification

#### 4.1.1 Theoretical Background on Two-Phase Pressure Drop Calculations

To calculate pressure drop on refrigeration cycles, different approaches and different techniques are used. These approaches are developed by combining experimental data and theoretical applications. Due to difficulties on 2 phase pressure drop calculations and its sub categories such as:

- Gravitational Pressure Drop
- Acceleration Pressure Drop
- Frictional Pressure Drop

Homogenous and heterogenous approaches are developed and theoretical pressure drop is obtained. While eliminating the answers on gravitational pressure drop and acceleration pressure would not make that much difference on to applications, frictional pressure drop could not converge to actual data as much as other pressure drop models.

To calculate frictional pressure drop accurately, different approaches are developed. These approaches are based on calculating the pressure drop for one phase – which is liquid- then multiplying one phase pressure drop by “two-phase multiplier”. Before proceeding to two-phase pressure drop models, let us examine general theoretical background on 2 phase flow.

## Mass Flow Rate ( $\dot{M}$ ) $(\frac{\text{kg}}{\text{s}})$

Mass Flow Rate is the summation of liquid mass flow rate on the mixture and gas mass flow rate.

$$\dot{M} = \dot{M}_l + \dot{M}_g \quad (1)$$

For some cases, mass flow can be given prior to process while most of the cases that is not possible. Sometimes it necessary to obtain mass flux with respect to inputs such as Capacity (kW) of the system and enthalpy reading for the given scenarios. The scenario will be given after vapor quality definition and the study will held.

## Vapor Quality ( $\dot{x}$ )

Vapor Quality  $\dot{x}$  is defined as the ratio of the vapor mass flow rate  $\dot{M}_g$   $(\frac{\text{kg}}{\text{s}})$  divided by the total mass flow rate  $(\dot{M}_g + \dot{M}_l)$

$$\dot{x} = \frac{\dot{M}_g}{\dot{M}} = \frac{\dot{M}_g}{\dot{M}_l + \dot{M}_g} \quad (2)$$

Let's define the scenario that mentioned previously:

- 40°C and 10°C subcooling on Condensation
- 0°C and 10°C superheating on Evaporation
- 10 kW System Capacity

In that case, by reading the figure on A-1 Appendix

- $h_f=200 \text{ kJ/kg}$
- $h_g=300 \text{ kJ/kg}$
- $h_2=243 \text{ kJ/kg}$
- $h_3=390 \text{ kJ/kg}$

$$h_2 = h_f + h_{fg} * \dot{x} \quad (3)$$

$$\dot{x} = \frac{(h_2 - h_f)}{h_{fg}} \quad (4)$$

$$\dot{x} = \frac{(243 - 200)}{(300 - 200)} = 0.43 \quad (5)$$

Now, let's go back to mass flow rate determination and state the total mass flow rate of the system. For:

$$\text{Capacity} = 10 \text{ kW} \quad (6)$$

$$\Delta h = h_3 - h_2' = 390 - 243 = 147 \left( \frac{\text{kJ}}{\text{kg}} \right) \quad (7)$$

$$\dot{M} = \frac{\text{Capacity}}{\Delta h} = \frac{10000}{147} = 68.027 \left( \frac{\text{kg}}{\text{s}} \right) \quad (8)$$

### Void Fraction ( $\epsilon$ )

The void fraction is one of the most critical quantities to determine in a two-phase flow. It specifies how much cross-sectional area each phase takes up. It is a crucial element in the computation of pressure drop, flow pattern transitions, and heat transfer coefficients since it specifies the mean velocities of the liquid and vapor.[11]

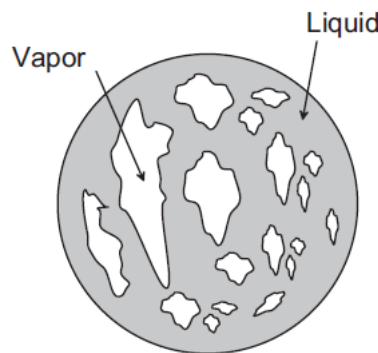


**Figure 18** Cross-Sectional Void Fraction

$$\epsilon_{homogenous} = \frac{\rho_l \dot{x}}{\rho_l \dot{x} + \rho_g (1 - \dot{x})} \quad (9)$$

Despite its simplicity, the homogeneous model can be used to build very excellent descriptions of gas–liquid fluxes provided it is applied correctly [12]:

- The phases are well mixed, as is the case downstream of fittings, for example.
- As is the case at high pressures, the changes between the phases are minor.

In all conservation equations involving gas–liquid fluxes, the void fraction must be taken into consideration. As a result, this quantity has been thoroughly explored. According to Zuber and Findly, several void fraction calculation algorithms are based on the drift-flux concept [13]. During this methodology Rouhani C. is used due to having mass flux higher than  $250 \left( \frac{kg}{m^2 s} \right)$

$$\epsilon = \left( \frac{C_o}{\epsilon_{hom}} + \frac{\rho_g u_{gj}}{\dot{x} \dot{m}} \right)^{-1} \quad (10)$$

Where;

Author		Application
Rouhani C. [8]	$C_0 = 1 + 0, 2 \cdot (1 - \dot{x}) \cdot \frac{(g d_h)^{0.25} \rho_l^{0.5}}{\dot{m}^{0.5}}$ $u_{gj} = 1, 18 \cdot \left( g \cdot \sigma \cdot (\rho_l - \rho_g) \right)^{0.25} \cdot (1 - \dot{x}) / \sqrt{\rho_l}$	Tubes and ducts for $\dot{m} > 250 \text{ kg/m}^2 \text{s}$
Morooka S., T. Ishi-zuka, M. Iizuka, K. Yoshimura [14]	$C_0 = 1, 08; u_{gj} = 3, 04 \cdot \left[ \frac{\sigma g (\rho_l - \rho_g)}{\rho_l^2} \right]^{0.25}$ $C_0 = 1, 13; u_{gj} = 1, 41 \cdot \left[ \frac{\sigma g (\rho_l - \rho_g)}{\rho_l^2} \right]^{0.25}$	Longitudinal flow through a bundle of tubes or fuel element for $\dot{m}/\rho_{hom} > 5 \text{ m/s}$ and $\varepsilon < 0, 9$ for $\dot{m}/\rho_{hom} < 5 \text{ m/s}$ and $\varepsilon < 0, 9$
Schrage D.E., J.-T. Hsu, M. K. Jensen [15]	$C_0 = (1 + 0, 36 \cdot \dot{m}^{-0.191} \cdot \ln(\dot{x}))^{-1}; u_{gj} = 0$ $\dot{m} \text{ in } \text{kg/m}^2 \text{s}$	Transverse flow through a bundle of tubes, guided flow, vertically upwards, medium R113 Valid for $\dot{m}$ values from 680 to 50
Margat, L, B. Thonon, L. Tadrist [16]	$C_0 = 0, 9636; u_{gj} = 0, 4275 \text{ for } \dot{m} = 125 \text{ kg/m}^2 \text{s}$ $C_0 = 0, 8831; u_{gj} = 0, 4296 \text{ for } \dot{m} = 85 \text{ kg/m}^2 \text{s}$ $C_0 = 0, 7552; u_{gj} = 0, 3453 \text{ for } \dot{m} = 37 \text{ kg/m}^2 \text{s}$	Plate heat exchanger, medium R134a

**Figure 19** Values for  $C_o$  and  $u_{gj}$  [14]

**Mass Flux (G) or ( $\dot{m}$ )  $\left( \frac{kg}{m^2 s} \right)$**

Mass Flux is the ratio of total mass flow rate divided by cross sectional area.

$$G_{pipe} = \dot{m} = \frac{\dot{M}}{A_{pipe}} \quad (11)$$

$$G_{tube} = \dot{m} = \frac{\dot{M}}{A_{Tube} * n_{circuit}} \quad (12)$$

**Velocity**  $\left(\frac{m}{s}\right)$

In two phase flow, there are different velocities that we use for different purposes.

True Average Velocity

$$u_g = \frac{\dot{x} \dot{M}}{\epsilon \rho_G A} = \frac{G \dot{x}}{\rho_G \epsilon} \quad (13)$$

$$u_g = \frac{1 - \dot{x}}{1 - \epsilon} \frac{\dot{M}}{\rho_l A} = \frac{G}{\rho_l} \frac{1 - \dot{x}}{1 - \epsilon} \quad (14)$$

$$u_m = u_g + u_l \quad (15)$$

Superficial Velocity

$$j_g = \frac{G}{\rho_G} \dot{x} = \epsilon u_g \quad (16)$$

$$j_l = \frac{G}{\rho_L} (1 - \dot{x}) = (1 - \epsilon) u_l \quad (17)$$

$$j_m = j_l + j_g \quad (18)$$

Lambda ( $\lambda$ ) is defined with respect to superficial velocity

$$\lambda = \frac{j_l}{j_l + j_g} \quad (19)$$

Density of the mixture is defined with respect to superficial velocity

$$\rho_{hom} = \rho_l \lambda + \rho_g (1 - \lambda) \quad (20)$$

and/or

$$\rho_{hom} = \rho_l (1 - \epsilon) + \rho_g \epsilon \quad (21)$$

#### 4.1.2 Dimensionless Number of Fluid Flow

The principal non-dimensional numbers used in the present study will be defined below. These non-dimensional numbers are used to determine characteristics of flow and develop new approaches.

##### Reynolds Number (Re)

$$Re_l = \frac{\rho_l u_l D_h}{\mu_l} \quad (22)$$

$$Re_g = \frac{\rho_g u_g D_h}{\mu_g} \quad (23)$$

If we express Re in terms of mass flux (G)

$$Re_l = \frac{G D_h (1 - \dot{x})}{\mu_l (1 - \epsilon)} \quad (24)$$

$$Re_g = \frac{G D_h (\dot{x})}{\mu_g (\epsilon)} \quad (25)$$

where

$D_h$  is the hydraulic diameter. In circular tubes  $D_h = D$

##### Nusselt Number (Nu)

$$Nu = \frac{h D}{\lambda_{th}} \quad (26)$$

Where

- $h$ = heat transfer coefficient
- $D$ =Tube Diameter
- $\lambda_{th}$ = Thermal Conductivity

##### Froude Number (Fr)

The Froude number is the proportion of inertia forces to gravitational forces.

$$Fr = \frac{u^2}{g L} = \frac{G^2}{\rho_l g D} \quad (27)$$

## Weber Number (We)

Weber Number represents the ratio of inertia to surface tension.

$$We_l = \rho_l u_l^2 \frac{D_h}{\sigma} \quad (28)$$

## Prandtl Number (Pr)

The Prandtl Number is the proportion of momentum diffusivity to thermal diffusivity.

$$Pr_l = \frac{c_{pl} \mu_l}{\lambda_l} \quad (29)$$

$$Pr_g = \frac{c_{pg} \mu_g}{\lambda_g} \quad (30)$$

## Martinelli Parameter

The Martinelli parameter is defined as the ratio of theoretical pressure gradients that would occur if either fluid flow alone in the pipe at its original flow rate. [11]

$$X_{tt}^2 = \frac{\left(\frac{\Delta P_F}{\Delta L}\right)_{lo}}{\left(\frac{\Delta P_F}{\Delta L}\right)_{go}} \quad (31)$$

$X_{tt}^2$  is void fraction independent and is a measure of the degree which states whether the two-phase mixture is closer to being liquid or gas. Two Phase multiplier that mentioned previously, is based on this parameter. Different correlations state their own multipliers. In the following pages, these multipliers will be handled.

Latest and most common use of Martinelli Parameter is:

$$\left(\frac{1 - \dot{x}}{x}\right)^{0.875} \left(\frac{\mu_l}{\mu_g}\right)^{0.125} \left(\frac{\rho_g}{\rho_l}\right)^{0.5} \quad (32)$$

## 4.2 Flow Regime Maps in Horizontal Tubes

Due to buoyancy forces, the liquid and vapor in a horizontal two-phase flow tend to separate, with the liquid moving to the bottom of the tube and the gas moving to the top.

Existed individual flow patterns are:

- Bubbly Flow
- Stratified Flow
- Stratified-Wavy Flow
- Intermittent Flow
- Plug Flow
- Slug Flow
- Annular Flow
- Mist Flow

Different flow pattern maps are developed to determine what type of pattern is existing for the given scenario. Most common and widely used map is created by Taitel and Dukler in 1976.

Taitel and Dukler's technique was based on a mechanistic investigation of flow transition mechanisms combined with a set of nondimensional characteristics. Their map has the axis of Martinelli Parameter X, gas Froude Number  $Fr_g$ , and parameters T and K. This map contains 3 axis and each of these axes has their own equations and curves.

Before proceeding to existed regime maps, let us examine how flow looks like in different regimes.

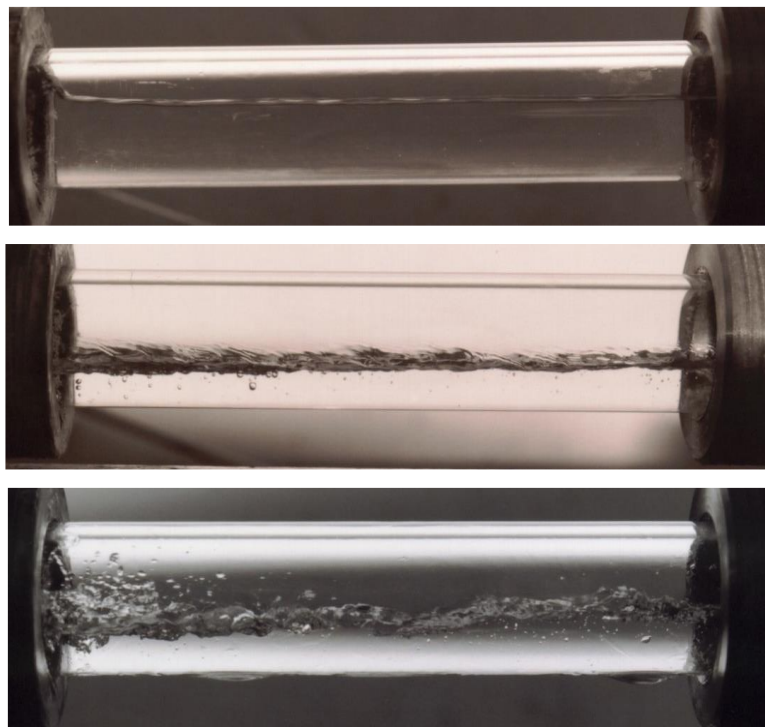


**Figure 20** a) Stratified Flow b) and c) Stratified Bubble Flow [15]

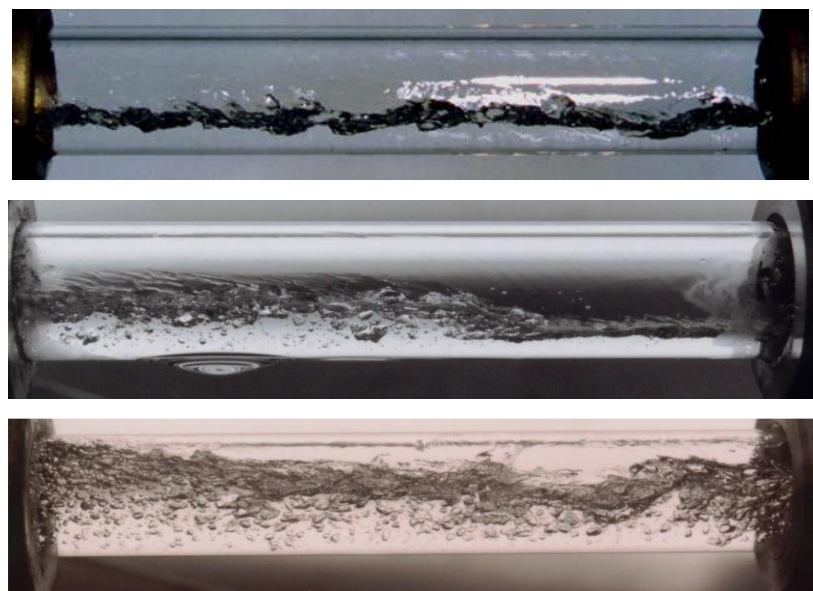


**Figure 21** Intermittent Flow Regime a) 9.52 mm Tube b) and c) 15.8 mm tube [15]

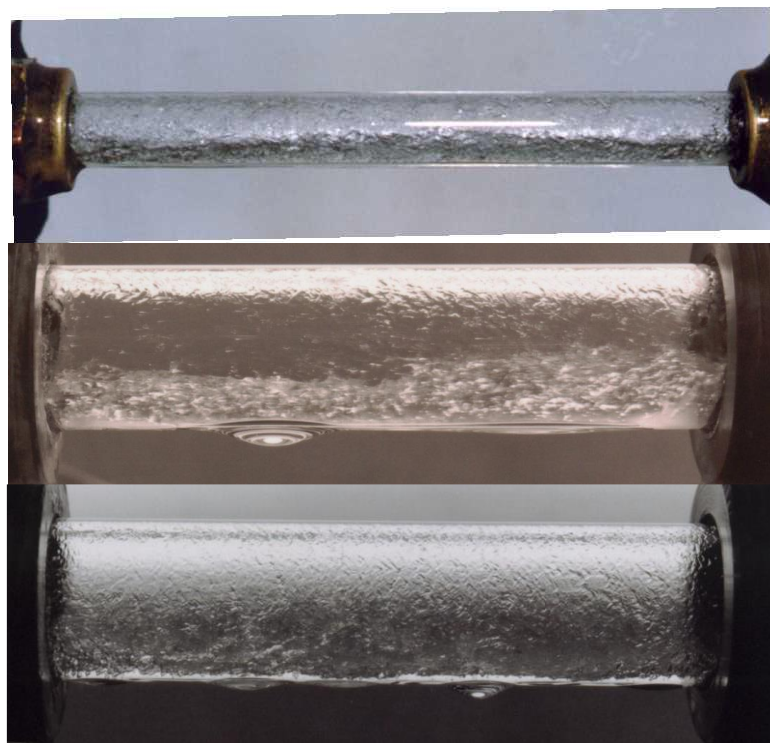


**Figure 22** Annular Flow Regime a) 9.52 mm Tube b) and c) 15.8 mm tube [15]

Figure 23 represent the flow pattern map according to Taitel and Dunkler for horizontal flow in tubes.

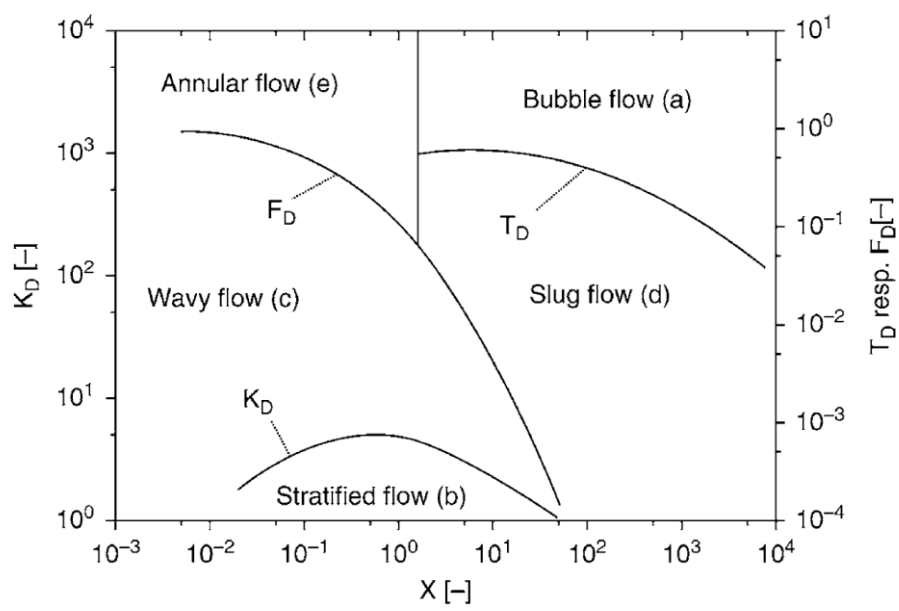


**Figure 23** Regime Map that belongs to Taitel and Dukler (1976)

Axis of given regime maps are:

- Martinelli Parameter (X)
- Gas Froude Number ( $Fr_g$ )
- Parameter T
- Parameter K

Martinelli Parameter is defined in eq. (31)

$$Fr_g = \frac{G_g}{(\rho_g(\rho_l - \rho_g) D g)^{1/2}} \quad (33)$$

$$T = \left[ \frac{\left| \frac{dp}{dz} \right|_l}{g (\rho_l - \rho_g)} \right]^{1/2} \quad (34)$$

$$K = Fr_g Re_l^{0.5} \quad (35)$$

Where

- $Re_l$  is eq. (24)
- $g$  = gravity  $\left( \frac{m}{s^2} \right)$

for  $Re_k < 2000$  Laminar flow characteristics are observed and,

$$f_k = \frac{16}{Re_k} \quad (36)$$

for  $Re_k > 2000$  Turbulent flow characteristics are observed and,

$$f_k = \frac{0.079}{Re_k^{1/4}} \quad (37)$$

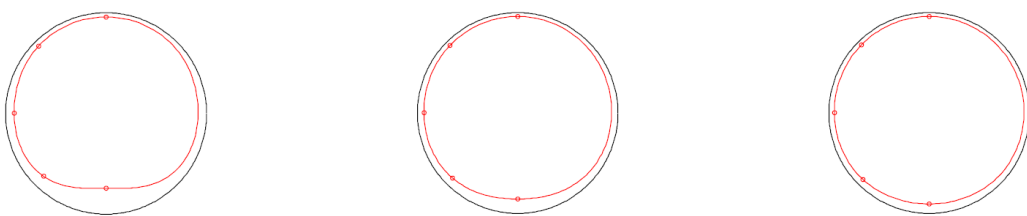


**Figure 24** a) Taitel and Dukler Two-phase flow pattern map b) asymmetric liquid film profiles c) Cioncolini and Thome updated version of regime map [15]

Since Taitel and Dukler (1976) regime map has three axis, to implement the map on the software, different techniques should be applied. Figure 25 represents the schematic of the applied map.

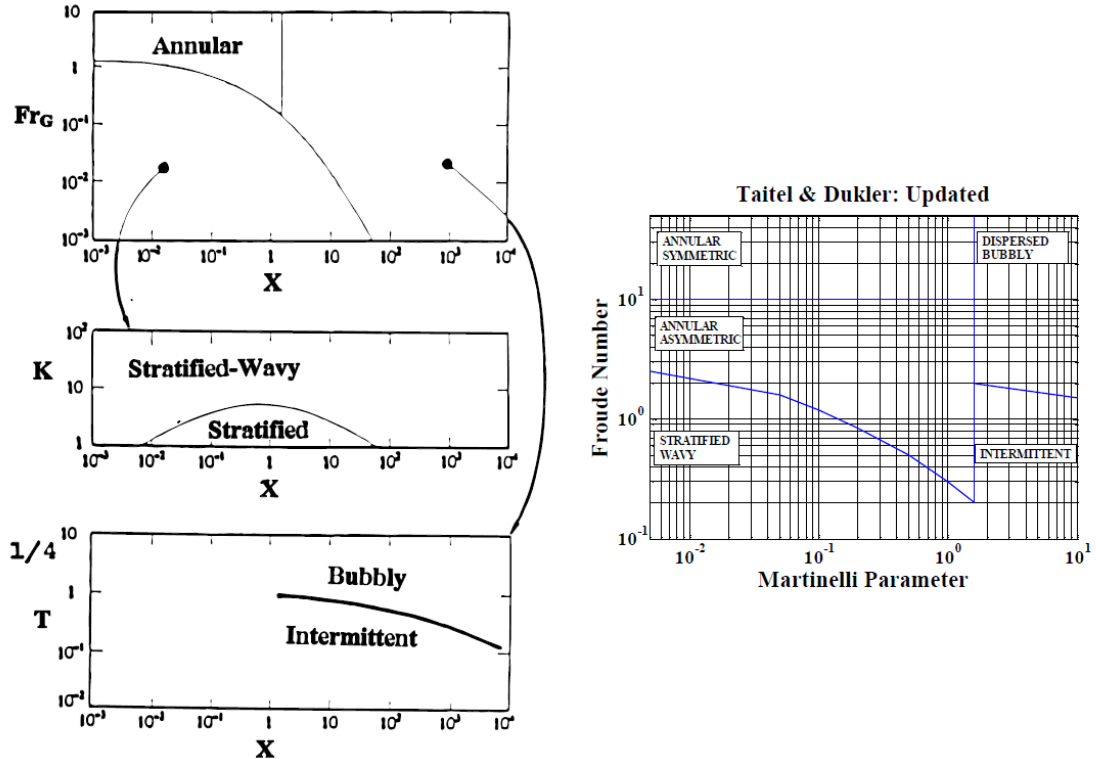


**Figure 25** Updated Version of Taitel & Dukler and its software implementation basis

To proceed the map, first we should determine Martinelli Parameter ( $X$ ) and  $Fr_g$ . By using these two parameters on the map, if their coordinates falling into annular area, then the regime has annular pattern.  $K$  is determined if the coordinates of  $X$  and  $Fr_g$  fall into the lower left zone of the map. The flow regime is classified as stratified-wavy or fully stratified using  $K$  and  $X$ . If the coordinates of  $Fr_g$  and  $X$  fall in the right zone on the top graph, then  $T$  is calculated. The flow regime is identified as either bubbly or intermittent using  $T$  and  $X$ . (plug or slug). The following equations were taken from their graph for its transition lines in order to incorporate this map into computer simulation. [15]:

For intermittent flow to bubbly flow:

$$Y = 1.056 X^{-0.070}; \text{ where } 2 \leq X \leq 50 \text{ and } 0.8 \leq Y \leq 1 \quad (38)$$

$$Y = -0.116 \ln(X) + 1.283; \text{ where } 50 \leq X \leq 9000 \text{ and } 0.2 \leq Y \leq 0.8 \quad (39)$$

For stratified flow to wavy flow:

$$Y = 1.405 \ln(X) + 7.521; \text{ where } 0.009 \leq X \leq 0.7 \text{ and } 1.0 \leq Y \leq 6.9 \quad (40)$$

$$Y = -1.337 \ln(X) + 6.620; \text{ where } 0.7 \leq X \leq 70 \text{ and } 1.0 \leq Y \leq 6.9 \quad (41)$$

For wavy flow to annular flow:

$$Y = 0.813 X^{-0.077}; \text{ where } 0.001 \leq X \leq 0.05 \text{ and } 0.95 \leq Y \leq 1.3 \quad (42)$$

$$Y = -0.214 \ln(X) + 0.305; \text{ where } 0.05 \leq X \leq 2 \text{ and } 0.17 \leq Y \leq 0.95 \quad (43)$$

$$Y = 0.412 X^{-1.188}; \text{ where } 2 \leq X \leq 12 \text{ and } 0.02 \leq Y \leq 0.17 \quad (44)$$

$$Y = 2.041 X^{-1.861}; \text{ where } 12 \leq X \leq 60 \text{ and } 0.001 \leq Y \leq 0.02 \quad (45)$$

For bubbly/intermittent flow to annular flow:

$$X = 2; \text{ where } 0.18 \leq Y \leq 0.10 \quad (46)$$

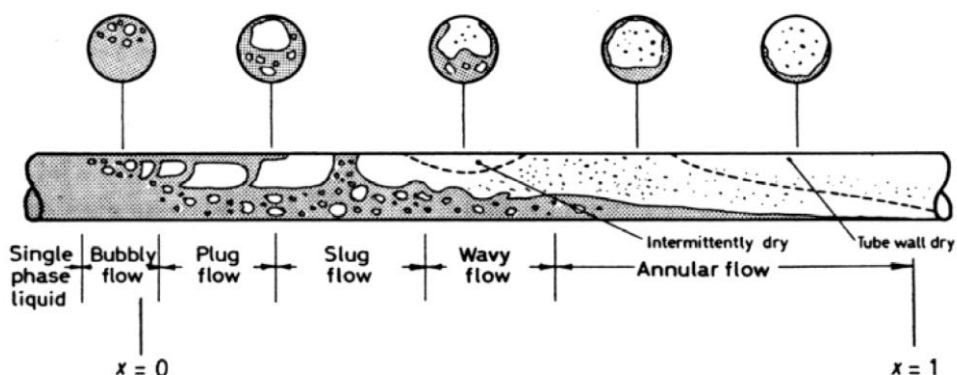


**Figure 26** Study of Collier and Thome (1994) existing flow patterns during evaporation

### 4.3 Two-Phase Pressure Drop Models

Despite the accurate theoretical calculations on single phase flow, numerous theoretical and experimental investigations do not yield a general model so far. The reason why still we cannot talk of a general two-phase flow model is related with having complexities, non-linearities, transition to turbulence and instabilities on two-phase flow characteristics. The study of two-phase flow analysis is held on three approaches:

- Empirical Correlations
- Phenomenological models
- Analytical Models

In fluid flow, total pressure drop is the summation of the variation of potential energy of the fluid, kinetic energy of the fluid and frictional loss on tube pipes. So, we can define total pressure drop  $\Delta P_{total}$  as the summation of

- Static pressure drop:  $\Delta P_{static}$  or  $\Delta P_{gravitational}$
- Momentum pressure drop:  $\Delta P_{momentum}$
- Frictional Pressure Drop:  $\Delta P_{frictional}$

Above pressure drops, refer to eq. (47)

$$\Delta P = \Delta P_{static} + \Delta P_{momentum} + \Delta P_{frictional} \quad (47)$$

For horizontal tubes, we cannot mention of  $\Delta P_{static}$  due to zero change in static head.

Momentum pressure drop - also known as acceleration pressure drop- can be calculated via.

$$\Delta P_A = [u_g^2 \rho_g \epsilon + u_l^2 \rho_l (1 - \epsilon)]_{out} - [u_g^2 \rho_g \epsilon + u_l^2 \rho_l (1 - \epsilon)]_{in} \quad (48)$$

Since there is no flow in but only out in distributor, eq. (48) becomes:

$$\Delta P_A = [u_g^2 \rho_g \epsilon + u_l^2 \rho_l (1 - \epsilon)]_{out} \quad (49)$$

After dealing with static and momentum pressure drop, frictional pressure drop comes next. Due to not working on single phase flow, there are some obstacles existed that needs to be overcome. To overcome this obstacles, different approaches are developed by different scientist. Before specifying the frictional pressure drop equation directly, we need to consider approaches and why they are not chosen for present study.

During this thesis study, different types of correlations, models and approaches are tried and taken into account. Advantages and disadvantages of these models are examined and empirical method is determined to use. Before proceeding what is used during software development, let me introduce existing approaches and why they are not chosen for present study.

#### **4.3.1 Analytical Methods**

Developing two phase flow model by considering analytical methods, requires iterative and numerical procedures which consume so much times. Since empirical techniques are not used in analytical methods, general solutions may occur and these solutions are not aimed to study due to their time disadvantage.

By considering analytical methods, some studies are development and it is possible to study these complex and non-time effective approaches. Despite the fact that the whole set of equations describing these models exists, I have chosen not to include them in my study due to their large size and the fact that I did not use these approaches throughout my research.

#### **4.3.2 Phenomenological Methods**

In the literature, developed two phase pressure drop models are existing. These approaches are based on phenomenological interfacial structure. So, it is taken into account, theoretically based approaches are used. Hence, they are not suitable for different flow regimes that emerges in general application methods. Whether they have this dominant advantage, empiric study is still required for this method and this is the biggest setback. There is also no universal flow pattern-based model available yet. They are, in fact, only available for specific flow patterns or flow structures. In literature, Bandel [16], Beattie and Whalley [17], Hashizume et al. [18] studies can be seen as studies for this approach. Since, non-existence of general solution and need of very reliable flow pattern map in order to be able predict the different interfacial structures, I did not consider none of these approaches in this study.

### **4.3.3 Empirical Methods**

Empirical methods on two-phase flow analysis are commonly used. What makes this method so unique and refer to its common use is minimizing the required knowledge of system characteristics. Hence, empirical methods are easy to integrate and they often provide good accuracy in the range of database which held for empiric studies. Database selection, such as tube materials, refrigerant properties etc. play crucial role on the development of empirical methods and so thus correlations. Due to empirical study base, disadvantage of this approach can be named as limited range of underlying database. We can also count that; no single correlation is able to provide good and accurate range for general sense.

So many studies are held on developing empirical correlation to analyze two-phase pressure drop in both horizontal and vertical tubes. Initial study in this area is done via Lockhart and Martinelli (1949) [19]. This work is still highly referenced on present studies. Later on, new studies with new underlying database are followed this study and Lockhart-Martinelli correlation is aimed to be taken a step forward.

In 1949, they stated that two-phase flow could be divided into four regimes:

- liquid viscous and gas turbulent (vt)
- liquid and gas both turbulent (tt),
- liquid and gas both viscous (vv)
- liquid turbulent and gas viscous (tv)

The critical points were chosen to be consistent with single-phase flow and to provide the best experimental data correlation. The analysis is based on two essential propositions:

- Regardless of the flow pattern, the static pressure drop for liquid and gaseous phases must be equivalent.
- At any point in time (position), the amount occupied by the liquid plus the gas must equal the entire volume of the pipe.

The flow pattern does not vary along the tube, according to these Lockhart-Martinelli propositions. They effectively prevent substantial pressure variations, such as slug and intermittent flows, as well as radial pressure gradients, such as stratified and stratified-wavy flows.

Then two-phase frictional pressure drop is modeled with the parameter which is called two phase multiplier.

$$\Delta P_{frictional} = \Phi_L^2 \Delta P_l \quad (50)$$

$$\Delta P_{frictional} = \Phi_g^2 \Delta P_g \quad (51)$$

where

- $\Delta P_l$ : Frictional pressure drop is the flow is liquid only
- $\Delta P_g$ : Frictional pressure drop is the flow is gas only

To calculate  $\Delta P_l$  and  $\Delta P_g$  followed equations is used.

$$\Delta P_l = 4f_{lo} \left(\frac{L}{D}\right) G^2 (1-x)^2 \left(\frac{1}{2\rho_l}\right) \quad (52)$$

$$\Delta P_g = 4f_{go} \left(\frac{L}{D}\right) G^2 x^2 \left(\frac{1}{2\rho_g}\right) \quad (53)$$

where

$$f_{lo} = \frac{0.079}{Re_{lo}^{0.25}} \quad \text{where} \quad Re_{lo} = \frac{G D (1-\dot{x})}{\mu_l} \quad (54)$$

$$f_{go} = \frac{0.079}{Re_{go}^{0.25}} \quad \text{where} \quad Re_{go} = \frac{G D \dot{x}}{\mu_g} \quad (55)$$

To complete eq. (50), we need to define Martinelli Parameter  $\Phi_L^2$  as well.

$$\Phi_L^2 = 1 + \frac{C}{X} + \frac{1}{X^2} \quad (56)$$

$$\Phi_L^2 = 1 + C X + X^2 \quad (57)$$

where C is:

**Table 1** C value that fits into Lockhart and Martinelli Equation

Liquid	Gas	Type	C
Turbulent	Turbulent	(tt)	20
Viscous	Turbulent	(vt)	12
Turbulent	Viscous	(tv)	10
Viscous	Viscous	(vv)	5

There are also other studies that is aimed to determine pressure drop on two-phase flow. To demonstrate,

- Bankoff [20]
- Cicchitti et al. [21]
- Thom [22]
- Pierr [23]
- Baroczy [24]
- Chisholm [25]
- Friedel [26]
- Müller-Steinhagen and Heck [27]

can be given as the correlations that are also available for this purpose.

After studying and examining all the given correlations above, Chisholm's approach is selected to put the study on a further step. Since, Chisholm transformed the graphical procedure of Baroczy [24] to enable a more convenient application to the case evaporating turbulent flow of two-phase mixtures in smooth tubes.

Baroczy (1966) suggested a graphical correlation for predicting the frictional pressure gradient, which could be applied to a wide range of gas-liquid combinations in practical applications. Chisholm (1973) was the first to establish empirical equations that resembled Baroczy's graphs, substantially simplifying the practical implementation of this correlation. The two-phase frictional pressure gradient is anticipated as a multiple of the single-phase liquid using this method. [28].

It's worth noting that, while the methodologies devised for smooth tubes agreed well with experimental air-water flow data in vertical channels, they drastically underestimated experimental air-water flow data in horizontal tubes.

Chisholm stated his two-phase frictional gradient as:

$$\Delta P_{friction} = \Phi_{Ch}^2 \Delta P_{lo} \quad (58)$$

The frictional pressure drops for the liquid and vapor phases are calculated same as Lockhart-Martinelli in eq. (52) and eq. (53)

The friction factors are obtained as in eq. (54) and eq. (55) for turbulent flow.

For laminar flow:

$$f = \frac{16}{Re_l} \quad (59)$$

Where the flow is considered

- fully turbulent at  $Re \geq 2000$
- laminar at  $Re < 2000$

Chisholm stated the parameter Y to obtain the ratio of the frictional pressure drop. That parameter Y is:

$$Y^2 = \frac{\Delta P_g}{\Delta P_l} \quad (60)$$

Chisholm defined his two-phase multiplier as follows:

$$\Phi_{Ch}^2 = 1 + (Y^2 - 1) \left[ B \dot{x}^{\frac{2-n}{2}} * (1 - \dot{x})^{(2-n)/2} + \dot{x}^{2-n} \right] \quad (61)$$

where n= 0.25 the exponent from the friction factor expression of Blasius.

The two-phase multiplier may be calculated after calculating the value of B, and hence the frictional pressure drop can be estimated using this method.

To make an end to Chisholm's correlation, he developed the parameters called Chisholm Parameters B.

for  $0 < Y < 9.5$

$$B = \frac{55}{G^{\frac{1}{2}}} \quad \text{for} \quad G \geq 1900 \quad (62)$$

$$B = \frac{2400}{G} \quad \text{for} \quad 500 \leq G \leq 1900 \quad (63)$$

$$B = \frac{55}{G^{\frac{1}{2}}} \quad \text{for} \quad G \leq 500 \quad (64)$$

for  $9.5 < Y < 28$

$$B = \frac{520}{Y * G^{\frac{1}{2}}} \quad \text{for} \quad G \leq 600 \quad (65)$$

$$B = \frac{21}{Y} \quad \text{for} \quad 600 \leq G \quad (66)$$

for  $Y > 28$

$$B = \frac{1500}{Y^2 G^{\frac{1}{2}}} \quad (67)$$

So, by the elimination of existing two-phase pressure drop models, they are considered with respect to their accuracies and advantages into each other. Chisholm Models is determined and with the integration of Chisholm's equations,  $\Delta P_{\text{friction}}$  is concluded and pressure drop that occurs in the tube has eliminated.

#### 4.4 Nozzle Pressure Drop

Nozzle pressure is expressed by  $\Delta P_N$ . Both inlet and outlet nozzles may be calculated by using

$$\Delta P_N = \zeta_N \frac{\rho w_N^2}{2} \quad (68)$$

where

- $\zeta_N$ : Nozzle Drag Coef.
- $w_N^2$ : Nozzle Velocity

To calculate  $w_N$ , we can either use

$$w_N = \frac{\dot{V}}{\frac{\pi}{4} d_N^2} \quad (69)$$

or

$$w_N = \frac{\dot{m}}{\rho_{mixture} \frac{\pi}{4} d_N^2} \quad (70)$$

This nozzle pressure drop equation is depends on the purpose of the analysis. While for jet nozzle the drag coefficient  $\zeta_N$  can be taken as 1, in heat exchangers  $\zeta_N$  supposed to be found via:

$$\zeta_N = 5.79 \left( \frac{A_N}{A_F} \right)^{1.14} \left[ \left( \frac{d_N}{D_i} \right) \left( \frac{D_{BE}}{d_N} \right)^{2.4} \right] \quad (71)$$

$$\left( \frac{A_N}{A_F} \right) = \frac{\frac{\pi}{4} d_N^2}{\frac{\pi}{4} (D_i - n_T d_o^2)} \quad (72)$$

where the bundle diameter  $D_{BE}$  is the diameter of a circle, which touches the outermost tubes of all tubes in the shell.  $D_{BE}=D_B$ .

In this study, nozzle pressure drop is found by using the following equation.

$$\Delta P_N = \frac{1}{2} \rho (1 - \beta^4) \left( \frac{w_n}{C_d} \right)^2 \quad (73)$$

Where

$$\beta = \frac{D_{nozzle}}{D_{pipe}} \quad (74)$$

$$w_n = \frac{\dot{M}}{\rho * A_{nozzle}} \quad (75)$$

And  $C_d$  is determined based on Table 2.

**Table 2** Cd Coefficient Table

Equipment Type	$C_d$
Orifice Plate, thin sharp edged	0.61
Venturi Nozzle, Machined	0.995
Venturi Nozzle, Rough Welded Sheet Metal	0.985
Venturi Nozzle, Rough Cast	0.984

for this study, machined venturi nozzle is used and  $C_d = 0.995$  is applied on the software.

## **5. EXPERIMENTEL SETUP**

### **5.1 Laboratory Explanation**

In Figure 27 and 28 calorimetric chamber and air-conditioning chamber is represented as the experimental setup.

Calorimetric room contains;

- a test room for evaporator and condenser
- a control unit for regulating the temperature and humidity
- refrigeration unit to control refrigerant velocity and temperature

The difference between calorimetric room and air-conditioning chamber is that calorimetric room is able to calculate suitable air capacity with respect to air flow rate by using the wind tunnel sensors. In testing of cooling devices with constant air flow rate, there is no need to specify the capacity because air capacity can be calculated with electrical loads.

In heat exchangers, there are inlet and outlet end of the piping systems. These piping systems takes role in order to charge or discharge the evaporator. Also, there are two existing sensors which takes place in the piping system in order to read inlet & outlet temperatures and pressure of the system.

Both calorimetric chamber and air-conditioning chamber contain air conditioning unit in order to control additional cooling capacity in condenser tests but not for evaporators. Air inlet temperature and humidity sensor works with respect to present temperature and humidity level in the chamber.

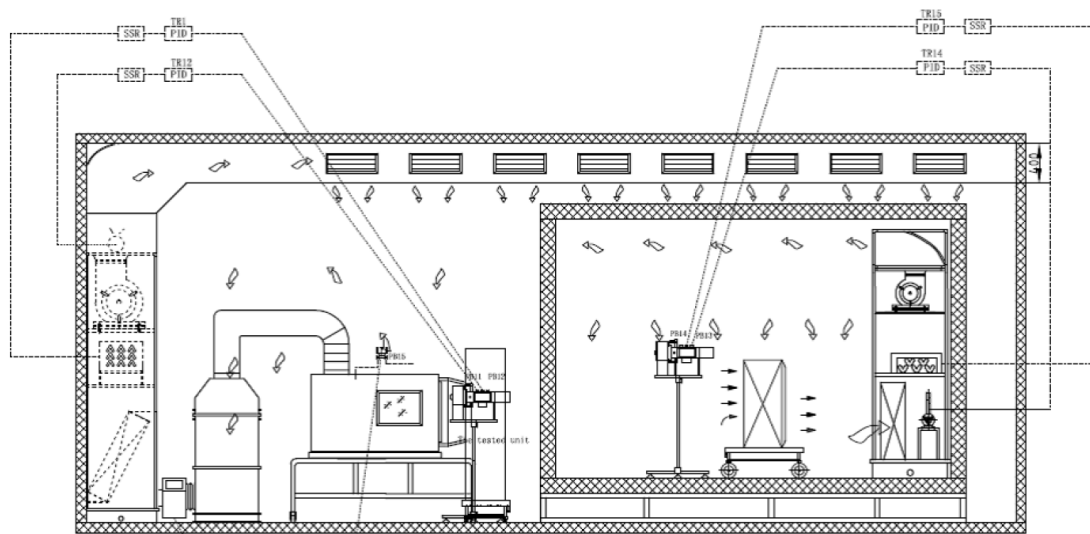


**Figure 27** Schematic Representation of the Experiment Setup. LHS Air-Conditioning Chamber and RHS Calorimetric Chamber



**Figure 28** a) Air-Conditioning Chamber b.) Calorimetric Chamber

During experimentation process, R404A is used as the refrigerant. Temperature control of the refrigerant and subcooling application in the condenser is given in Figure 29. Also, for condensation, body type condenser and for evaporation, evaporator is existing to control their pressure.

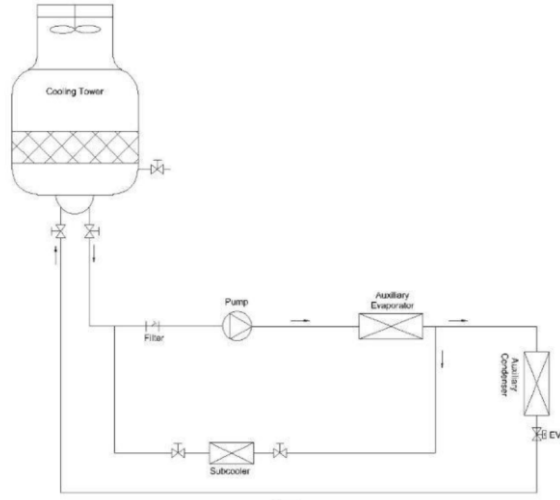


**Figure 29** Schematic Representation of Water Line

The selection of the expansion valve is very important in evaporator tests, this device is in the evaporator, significantly affect the characteristics of the flow. In this thesis study, electronic expansion valve (EXV) is used.

In figure 30, superheat control process on the evaporator, expansion valve and compressor path are adjusted by using measurement sensors.

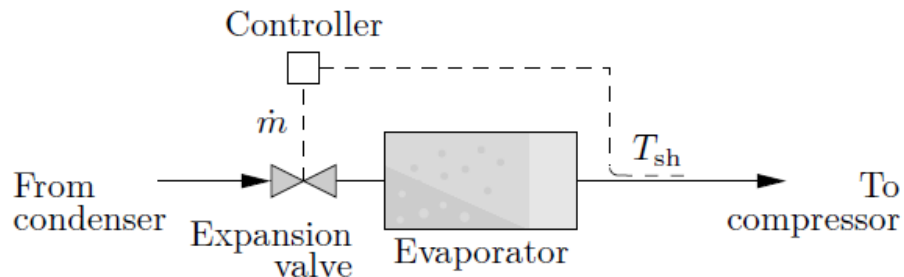


**Figure 30** Superheat Control Scheme

## 5.2 Electronic Control Principles

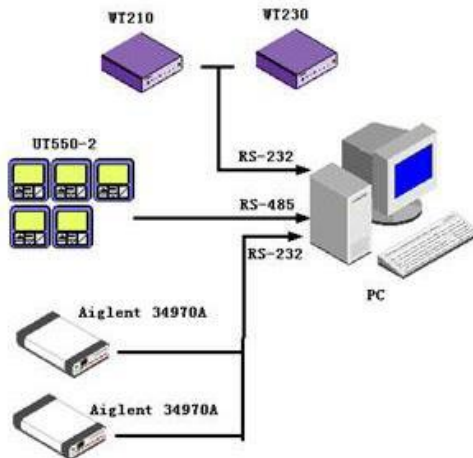


**Figure 31** Measurement System Schematic

The schematic of measurement system is given in Figure 31. Data obtained from measurement systems are studied on the devices which are given in Figure 31 and integrated with the computer software. In electronic setup, two Agilent 34970A model datalogger is measuring the system with the specified time frequency. Then, storing and analyzing the obtained data. In table 3 range of the measurement systems and their % error are represented.

**Table 3** Properties of Measurement Devices

Measured Property	Measurement Device	Measurement Range	Sensitivity
Temperature	K type thermocouple	-50 & 500 °C	± 0.3
Pressure	Pressure Transmitter	0-50 Bar	± 0.3
Humidity	Hygrometer	0-100 %	± 0.3
Mass Flow	Flowmeter	0-500 kg/h	± 0.6

Experimental properties which are voltage, current, electrical energy consumption, heat transfer capacity during the experiment in the calorimetric chamber, is measure via Yokogawa WT210 / 230 model -as in figure 32- digital power detector. Whereas WT210 model power detector is the only device that conducts the fan measurements, WT230 3 phase model is used to measure the properties of temperature and humidity units in the chamber.



**Figure 32** Agilent 34970A datalogger and Yokogawa WT210 Digital Power Measurement Device

The measurement held in the Friterm Thermal Devices Inc. laboratory is two-level system as shown in figure 33.

The first power supply system is the main power current braking (stopping) and AC contactor (closes open contacts and opens closed contacts by energizing the coil, electromagnetic switch that allows remote control) is fed. This control level is connected with all the existing electrical equipment in the scheme. PLC (Programmable Logical Controller) manages the on/off output signals of AC contactors, with HMI (Human Machine Interface is between the automation system realized using PLC systems and the user interacting unit) control equipment is managed. The second one is the capacity control. With this control system, heaters, humidifiers, valves, pumps need to be precisely controlled and adjusted and the fan is controlled. From PC with DDC (digital direct controller) or manually set values, signal PV (dynamic process value) is returned during sensor setting, Thus, with the PID algorithm, the actuator (which controls a mechanism or system or an analog signal is sent for a kind of engine that drives the engine. This signal is based on the DDC output value and it controls the equipment.

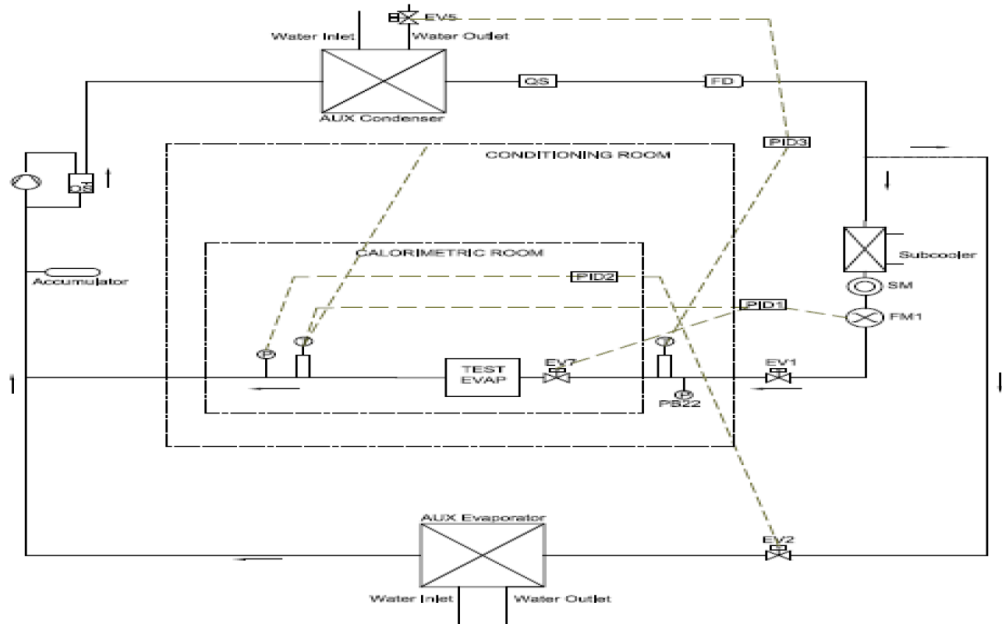


**Figure 33** PID Scheme of the Experimental Setup

To demonstrate, if the figure is to be examined; According to EV7 electronic expansion valve in PID1 evaporator outlet and test drive manual refrigerant flow in switch as FM1 is being set. In EV2 electronic expansion valve (located on the auxiliary line in PID2 valve) the tested evaporator pressure is adjusted. Before expansion valve in PID3 temperature in the electronic expansion valve at the hot water outlet on the auxiliary line is adjusted with the EV5.

### 5.3 Experiment Sample

In figure 34, provided experimental data sheet by Friterm, is given.

**FRITERM Termik Cihazlar San. Ve Tic. A.S.**  
  
**Unitary Air-cooler Performance Test Data**

Test Time 2021-7-8 9:23:58 Print Time 2021-7-8 14:03:18

Coil type	Evaporator	Project no	FES 1F2 30 4 4 SM	Model nam	
Order no	20210780-07	Exchange surface area		Fan model	EBM S4E300=AS72
Software capacity	exp valf Ex5	Software dFluid		Geometry	35x35 12mm CG
NTxNRxNC	12x4x4	Length x Fin pitch	1600x4	TT & FT	0.32x0x.15
<b>SC1_Air Cooler (Ref.)</b>					
Temp. Before EXPV	30 °C	Ref. flow	0.8 kg/h		
Evaporator/ Condenser Outlet Temp.	6.5 °C	Evaporating Pressure	0.60033 MPa		
Calorimeter Inlet DB	10 °C	Calorimeter Inlet DP	-3 °C		
Cond. Room Air Inlet DB	10.01 °C	1	2	3	4
Cond. Room Air Inlet DP	-5.51 °C	-5.48	-5.44	-5.42	-5.46
Calo. room air inlet DB	10.04 °C	10.03	10.02	10.03	10.03
Calo. room air inlet DP	-4.17 °C	-4.18	-4.20	-4.20	-4.19
Calo. room air outlet DB	5.53 °C	5.57	5.55	5.54	5.55
Coarse-adjusting temp.	25.20 °C	25.19	25.19	25.19	25.19
Inlet Relative Humidity	% 34.84	34.83	34.81	34.78	34.82
Refrigerant outlet temp of evaporator	6.58 °C	6.54	6.54	6.44	6.53
Refrigerant inlet temp of evaporator	13.91 °C	13.91	13.87	13.84	13.88
Evaporation pressure	MPa 0.601	0.602	0.602	0.598	0.601
Evaporation/Condensation temp	°C 0.02	0.07	0.07	-0.10	0.01
Temp. before expansion valve	36.67 °C	36.69	36.73	36.78	36.72
Pressure before expansion valve	MPa 1.93	1.94	1.93	1.93	1.93
Evaporator superheating	Kelvin 6.56	6.47	6.47	6.54	6.51
Liquid SC before EXPV (Ref.)	°C 5.56	5.78	5.60	5.46	5.60
Inlet vapor quality of refrigerant	0.33	0.33	0.33	0.33	0.33
Calo. Wall inside temp.	10.34 °C	10.32	10.32	10.32	10.33
Calo. Wall outside temp.	9.74 °C	9.76	9.77	9.78	9.76
Calo. room AHU fluid inlet temp.	10.96 °C	10.95	10.96	10.96	10.96
Calo. room AHU fluid outlet temp.	10.02 °C	10.02	10.03	10.03	10.03
Refrigerant pressure drop	kPa 334.671	334.868	333.330	336.639	334.877
DMP1 Voltage	V 227.51	227.63	227.37	227.84	227.59
DMP1 Current	A 1.37	1.37	1.37	1.37	1.37
DMP1 Watt	W 296.33	295.33	295.33	295.33	295.58
DMP2 ?? Voltage	V 388.94	389.64	389.99	388.90	389.37
DMP2 ?? Current	A 13.42	13.74	13.72	13.71	13.65
DMP2 ?? Watt	W 8386.67	8616.67	8576.67	8550.00	8532.50
Energy Supply To Calo.Room	kJ 20948.40	20940.84	20922.84	20897.28	20948.40
Refrigerant outlet enthalpy	kJ/kg 370.844	370.784	370.788	370.764	370.795
Refrigerant inlet enthalpy	kJ/kg 252.957	252.982	253.045	253.132	253.029
Fluid volumetric flow	m³/h 0.003	0.002	0.003	0.003	0.003
Refrigerant mass flow	kg/h 271.533	271.167	270.267	270.267	270.808
Refrigerant side capacity	kW 8.892	8.873	8.839	8.831	8.859
Calo. room capacity	kW 8.69	8.69	8.68	8.67	8.68
Thermal balance coefficient	% -2.33	-2.12	-1.83	-1.87	-2.04
Conclusion		Remark			

Tested by:

Reviewed by:

Approved by:

**Figure 34** Experiment Sample that Provided by Friterm

## 5.4 Theoretical Validation Setup: Commercial Software

To validate written software, two different methods are applied. First and most important validation is proceeded via considering experimental data and its evaluation.

Second and another important validation is held via using American Based commercial two-phase pressure drop software. As long as the presence of this thesis is based on not being able to have accurate result on this prior software, it is commonly used in the industry. Therefore, we consider to proceed evaluation with two different approaches.

Opening page of the software is given in Figure 34.



**Figure 35** Commercial Software

The interface of commercial software is shown in Figure 35.

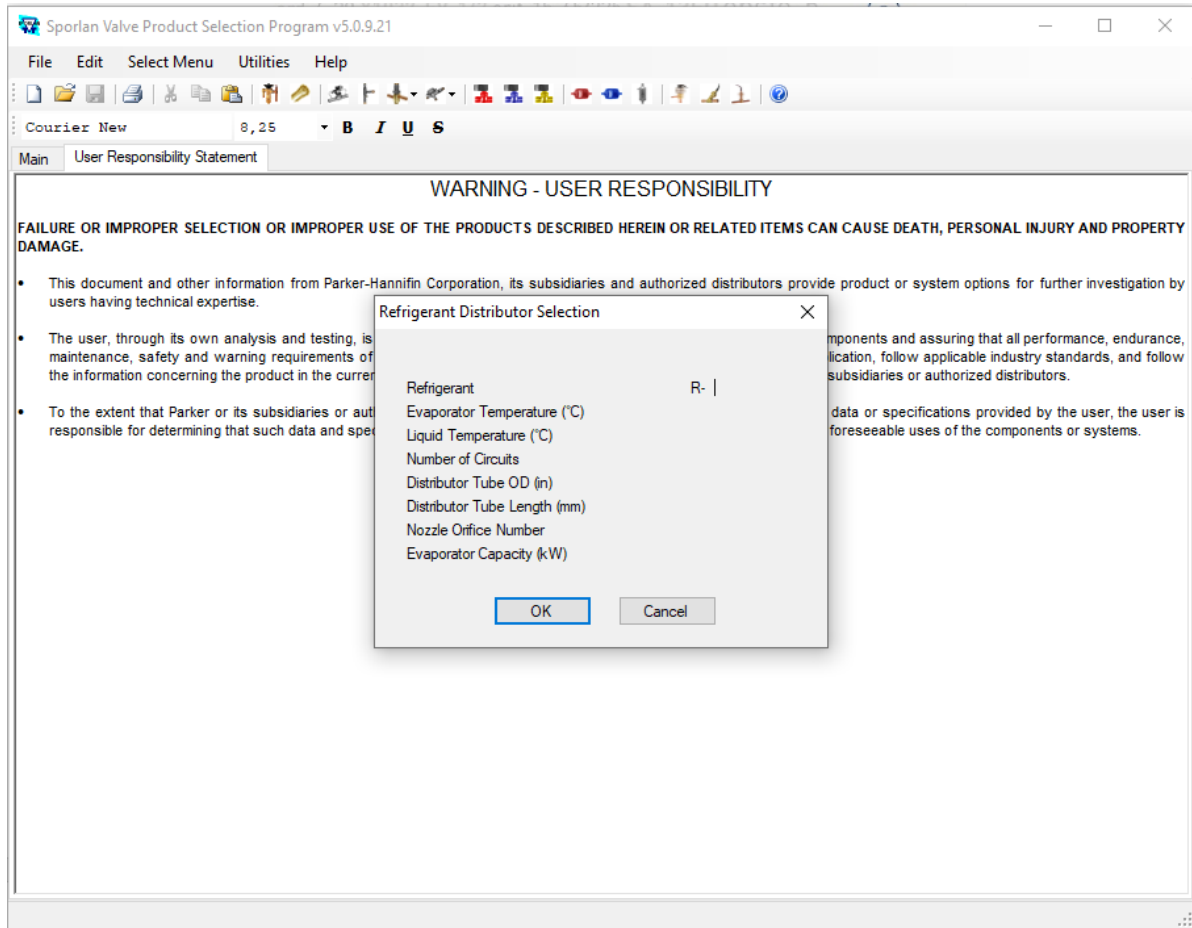


**Figure 36** Commercial Software Interface

By writing the desired system properties such as:

- Refrigerant
- Evaporator Temperature
- Liquid Temperature
- Number of Circuits
- Distributor Tube ID
- Distributor Tube Length
- Nozzle Orifice Number
- Evaporator Capacity

We get pressure drop output in terms of bar. The output interface is given in Figure 36.

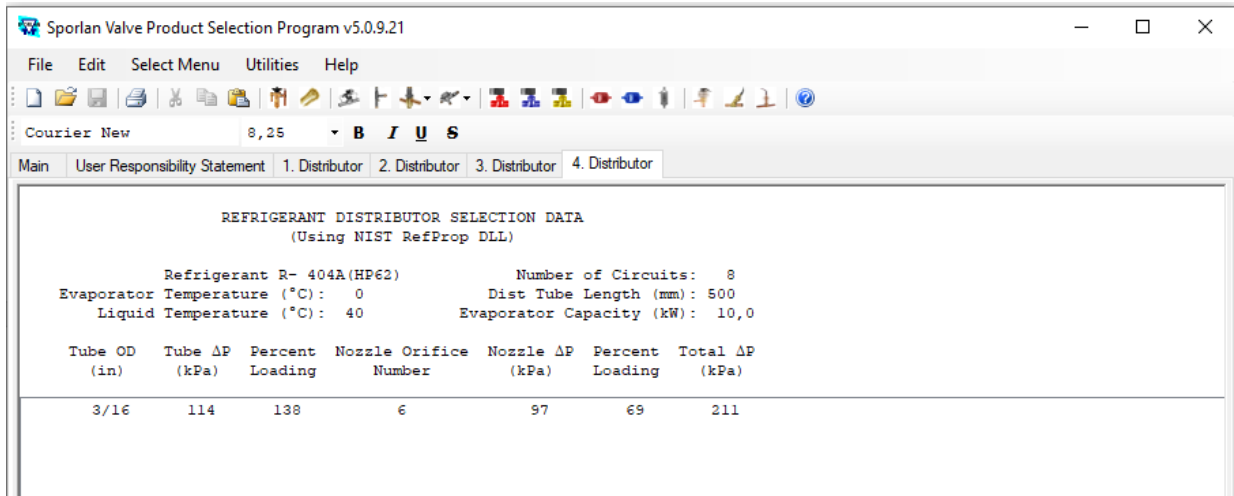


**Figure 37** Output Interface of the Existing Software

So, the evaluated result is existed for the following properties

- Refrigerant: R-404A
- Evaporator Temperature: 0 °C
- Liquid Temperature: 40 °C
- Number of Circuits: 8
- Distributor Tube ID: 3/16 inch
- Distributor Tube Length: 500 mm
- Nozzle Orifice Number: 6
- Evaporator Capacity: 10 kW

The outputs and their comparisons with thesis study will be evaluated in the following sections.

## **6. Developed Two Phase Pressure Drop Software**

Developed software is a combination of CoolProp, Phyton and MATLAB. Whereas the CoolProp and Phyton takes role at a small piece of all work, MATLAB is the main contractor.

Software development can be analyzed under two categories. These categories are:

- Refrigerant property integration
- Correlations and mathematical integration

### **6.1 Refrigerant Property Integration**

At first, CoolProp High Level Interface with documentation of 6.4.1 is downloaded to computer. Then Phyton -Anaconda extension- setup is proceeded. The reason why we need phyton is, CoolProp does not provide direct contact between MATLAB and their refrigerant property software. Hence, CoolProp & Phyton are introduced first, then MATLAB is combined with that software.

Making the software on CoolProp base, benefit us:

- Making our database smaller

If refrigerant properties were taken out of EES, Refprop or any related software, we would need extra database and data evaluation process for each refrigerant. By combining them, this time consumer process is evaluated and time saved for the user.

- Chance of having vast options on Refrigerant selection

Developed software can use for every fluid assigned on CoolProp High Level User Interface. That allow the software to work for new updated refrigerant properties and consider most updated data.

- Minimizing extra calculations

EES and Refprop does not give density, viscosity,  $c_p$ ,  $c_v$  for the quality between 0-1. These softwares only provide information for  $x=0$  and  $x=1$ . So thus, we would need to make extra interpolation on calculating the density, viscosity and other parameter of the two-phase fluid. Since CoolProp High Level User Interface provide us any type of

existing property in two-phase flow, the software does not need to do any extra work such as interpolation.

To check whether CoolProp is running successfully or not, different refrigerants in different temperatures are chosen and the data obtained from CoolProp and EES are compared. Since EES does not give 2phase quality between  $x=0$  and 1, i found homogenous density by using superficial velocity and density approaches given in eq. (19) and eq. (20)

So, fluid properties are obtained by using the given method and validation of method is conducted via data comparison on CoolProp.

## 6.2 Interface Creation

A total work of 1600 line code, is resulted as the default interface as given in Figure 37. Detailed Representation of the interface is given in Appendix.



**Figure 38** Software Interface

Software Consists of two separate bodies and two separate Run Button.

**Figure 39** Upper Body of the Interface

This part, is responsible of user defined inputs. User, start by selecting the refrigerant, selecting the tube inner diameter in terms of inch and assigning tube wall thickness with respect to the system that s/he would like to work.

Second section of upper body -Refrigerant Property Tree- refers condensation and evaporation temperatures of the working fluid. In addition, sub cooling and superheating is applied on the system to provide extra work zone compared to existing software.

Third section of the upper body- Distributor Tree- refers the properties of the distributor that user would like to study. This section starts by number of circuits, distributer tube length, nozzle orifice number, inlet pipe diameter and evaporator capacity.

When Run button – white background black font- is clicked, refrigerant property in the distributor will appear in the lower body of the interface. The lower body is given in

**Figure 40** Lower Body of the Interface

Figure 39.

Output Tree starts with

- $T$  °C
- $\dot{x}$
- Pressure (kPa)
- Density  $\rho$  (kg/m<sup>3</sup>)
- Enthalpy (h) (kj/kg)
- Heat Capacity at Constant Pressure ( $c_p$ )
- Heat Capacity at Constant Volume ( $c_v$ )
- Critical Pressure  $P_{crit}$
- Saturation Pressure
- Critical Temperature  $T_{crit}$
- Saturation Temperature
- Viscosity ( $\mu$ ) (Pa\*s)

When 2<sup>nd</sup> Run button- grey background white font- is clicked, refrigerant properties and distributor properties are matched, assigned correlations are used and pressure drop is evaluated.

At this section,

- Nozzle Percent Loading
- Nozzle Pressure Drop
- Tube Percent Loading
- Tube Pressure Drop
- Total Pressure Drop

is existing.

Also, check box and logo of Marmara University and Friterm A.Ş is existing at the right bottom.

Check box become green when the process is satisfied without error, and it becomes red if there is any missing part in input tree or any other possible errors.

## 6.3 Implemented Codes on Interface

### 6.3.1 Upper Body and Code Transformation between Run Buttons

When we come to background of the existing codes, at first MATLAB App Designer Property section is seen. This section works as the bridge between two different run buttons.

```
properties (Access = private)
    ref % refrigerant
    dia_t % tube dia
    Tliq % liquid input temp
    Tliq_i % liquid temp without subcooling
    Tevap % evaporation temp
    Tevap_i %
    xn % Quality
    P % Pressure
    rho % Density
    h2 % enthalpy at x=0.3 and T=Tliq
    h3 % enthalpy at x=1 and T=Tevap
    Pcrit %
    Psat %
    Tcrit %
    Tsat %
    V % Viscosity
end
```

**Figure 41** Property Callback Codes

This section help user to send properties between upper body and lower body. By the codes given above, data transformation and conduction are implemented.

After property transformation, input codes are coming, since I do not want to put so many messy bridge codes on the report, i would like to represent refrigerant observation codes that co-operate with CoolProp High Level Interface.

```
%%%%%% Refigerant Reading Loop
if (strcmp(app.RefrigerantSelectionDropDown.Value, 'R134A'))
    app.ref='(R134A)';
elseif (strcmp(app.RefrigerantSelectionDropDown.Value, 'R22'))
    app.ref='(R22)';
elseif (strcmp(app.RefrigerantSelectionDropDown.Value, 'R407C'))
    app.ref='(R407C.mix)';
elseif (strcmp(app.RefrigerantSelectionDropDown.Value, 'R410A'))
    app.ref='(R410A.mix)';
elseif (strcmp(app.RefrigerantSelectionDropDown.Value, 'R422D'))
    app.ref='(R422D.mix)';
elseif (strcmp(app.RefrigerantSelectionDropDown.Value, 'R404A'))
    app.ref='(R404A.mix)';
elseif (strcmp(app.RefrigerantSelectionDropDown.Value, 'R422A'))
    app.ref='(R422A.mix)';
elseif (strcmp(app.RefrigerantSelectionDropDown.Value, 'R507'))
    app.ref='(R507A.mix)';
elseif(strcmp(app.RefrigerantSelectionDropDown.Value, 'R1234 yf'))
    app.ref='(R1234yf)';
elseif (strcmp(app.RefrigerantSelectionDropDown.Value, 'R1234 ze'))
    app.ref='(R1234ze(E))';
elseif (strcmp(app.RefrigerantSelectionDropDown.Value, 'R448 A'))
    data=readtable('R448A.xlsx');
elseif (strcmp(app.RefrigerantSelectionDropDown.Value, 'R449 A'))
    app.ref='(R449A.mix)';
elseif (strcmp(app.RefrigerantSelectionDropDown.Value, 'R32'))
    app.ref='(R32)';
elseif (strcmp(app.RefrigerantSelectionDropDown.Value, 'R717'))
    app.ref='(R717)';
elseif (strcmp(app.RefrigerantSelectionDropDown.Value, 'R744'))
    app.ref='(R744)';
end
```

**Figure 42** Refrigerant Data Conduction Codes

- mass flow rate calculation follows this process:

```
%%%%%% Mass Flow Rate-Quality Calculation
P1=py.CoolProp.CoolProp.PropsSI('P', 'T',app.Tliq_i, 'Q', xf, app.ref);
if sub_c==0
app.h2=py.CoolProp.CoolProp.PropsSI('H', 'P', P1, 'Q', xf, app.ref);
else
app.h2=py.CoolProp.CoolProp.PropsSI('H', 'T',app.Tliq, 'P', P1, app.ref);
end

P3=py.CoolProp.CoolProp.PropsSI('P', 'T',app.Tevap_i, 'Q', xg, app.ref);
hf=py.CoolProp.CoolProp.PropsSI('H', 'T',app.Tevap_i, 'Q', xf, app.ref);
hg=py.CoolProp.CoolProp.PropsSI('H', 'T',app.Tevap_i, 'Q', xg, app.ref);
if sup_h==0
app.h3=py.CoolProp.CoolProp.PropsSI('H', 'P', P3, 'Q', 1, app.ref);
else
app.h3=py.CoolProp.CoolProp.PropsSI('H', 'T',app.Tevap, 'P', P3, app.ref);
end

hfg=hg-hf;
x=(app.h2-hf)/hfg;
```

**Figure 43** Mass Flow Rate Calculation Codes

- then, refrigerant properties are observed with:

```
%%%%%%%%%%%%%%%%%%%%%%%%%%%%%%%%%%%%%% Refrigerant Properties

app.Tliq=app.Tliq-273.15;
app.P=py.CoolProp.CoolProp.PropsSI('P', 'T',app.Tevap_i, 'Q', x, app.ref);
%app.rho=py.CoolProp.CoolProp.PropsSI('D', 'T',app.Tevap, 'Q', x, app.ref);
app.rho=py.CoolProp.CoolProp.PropsSI('D', 'T',app.Tevap_i, 'Q', x, app.ref);
%app.h=py.CoolProp.CoolProp.PropsSI('H', 'T',app.Tevap, 'Q', x, app.ref);
cp=py.CoolProp.CoolProp.PropsSI('Cpmass', 'T',app.Tevap_i, 'Q', x, app.ref);
%cp=py.CoolProp.CoolProp.PropsSI('Cpmass', 'T',app.Tevap, 'Q', x, app.ref);
cv=py.CoolProp.CoolProp.PropsSI('Cvmass', 'T',app.Tevap_i, 'Q', x, app.ref);
%cv=py.CoolProp.CoolProp.PropsSI('Cvmass', 'T',app.Tevap, 'Q', x, app.ref);
if (strcmp(app.RefrigerantSelectionDropDown.Value, 'R449 A'))
    app.Pcrit=4500000;
elseif (strcmp(app.RefrigerantSelectionDropDown.Value, 'R422D'))
    app.Pcrit=3905000;
elseif (strcmp(app.RefrigerantSelectionDropDown.Value, 'R422A'))
    app.Pcrit=3748000;
elseif (strcmp(app.RefrigerantSelectionDropDown.Value, 'R407C'))
    app.Pcrit=py.CoolProp.CoolProp.PropsSI("Pcrit","R407C");
elseif (strcmp(app.RefrigerantSelectionDropDown.Value, 'R410A'))
    app.Pcrit=py.CoolProp.CoolProp.PropsSI("Pcrit","R410A");
else
    app.Pcrit=py.CoolProp.CoolProp.PropsSI('Pcrit', 'T',app.Tevap_i, 'Q', x, app.ref);
end
app.Psat=py.CoolProp.CoolProp.PropsSI('P', 'T',app.Tevap_i, 'Q', x, app.ref);
if (strcmp(app.RefrigerantSelectionDropDown.Value, 'R449 A'))
    app.Tcrit=82.05+273.15;
elseif (strcmp(app.RefrigerantSelectionDropDown.Value, 'R422D'))
    app.Tcrit=79.6+273.15;
elseif (strcmp(app.RefrigerantSelectionDropDown.Value, 'R422A'))
    app.Tcrit=71.7+273.15;
elseif (strcmp(app.RefrigerantSelectionDropDown.Value, 'R407C'))
    app.Tcrit=py.CoolProp.CoolProp.PropsSI("Tcrit","R407C")-273.15;
elseif (strcmp(app.RefrigerantSelectionDropDown.Value, 'R410A'))
    app.Tcrit=py.CoolProp.CoolProp.PropsSI("Tcrit","R410A")-273.15;
else
    app.Tcrit=py.CoolProp.CoolProp.PropsSI('Tcrit', 'T',app.Tevap_i, 'Q', x, app.ref);
end
app.Tsat=py.CoolProp.CoolProp.PropsSI('T', 'P',P3, 'Q', x, app.ref);
%app.Tsat=py.CoolProp.CoolProp.PropsSI('T', 'T',app.Tevap, 'Q', x, app.ref);
app.V=py.CoolProp.CoolProp.PropsSI('V', 'T',app.Tevap_i, 'Q', x, app.ref);
%app.V=py.CoolProp.CoolProp.PropsSI('V', 'T',app.Tevap, 'Q', x, app.ref);
```

**Figure 44** Refrigerant Property Codes

- Diameter loop takes place

```
%%%%%%%%%%%%%%%%%%%%%%%%%%%%%%%%%%%%%% Dia Loop

if (strcmp(app.TubeIDinDropDown.Value, '3/16'))
    app.dia_t=4.7625; %mm
    %th=0.762; %mm
elseif (strcmp(app.TubeIDinDropDown.Value, '1/4'))
    app.dia_t=6.35; %mm
    %th=0.762; %mm
elseif (strcmp(app.TubeIDinDropDown.Value, '5/16'))
    app.dia_t=7.9375; %mm
    %th=0.8128; %mm
elseif (strcmp(app.TubeIDinDropDown.Value, '3/8'))
    app.dia_t=9.525; %mm
    %th=0.8128; %mm
end

th=app.TubeWallThicknessmmEditField.Value;
app.dia_t=(app.dia_t-2*th)*10^-3; %meter
```

**Figure 45** Diameter Elimination Codes

- To complete first run button, refrigerant properties are extracted to lower body of the interface with the given codes.

```
%%%%%%%%%%%%%%%%%%%%%%%%%%%%%%%%%%%%%% Property Panel
app.xn=x; %% This one is created to take x to next callback
app.TCEditField.Value=app.Tevap_i-273.15;
%app.TCEditField.Value=app.Tliq;
app.xEditField.Value=x;
app.PkPaEditField.Value=app.P*(10^-3);
app.Densitykgm3EditField.Value=app.rho;
%app.EnthalpykjkEditField.Value=app.h3*(10^-3);
app.EnthalpykjkEditField.Value=app.h2*(10^-3);
app.CpkjkkgEditField.Value=cp*(10^-3);
app.CvkjkkgEditField.Value=cv*(10^-3);
app.PcritkPaEditField.Value=app.Pcrit*(10^-3);
app.PsatkPaEditField.Value=app.Psat*(10^-3);
app.TcritCEditField.Value=app.Tcrit-273.15;
app.TsatCEditField.Value=app.Tsat-273.15;
app.ViscosityPAsEditField.Value=app.V;
```

**Figure 46** Answer Representation Codes

- Last section represent error box and initial Run button completes.

```
%%%%%%%%%%%%%%%%%%%%%%%%%%%%%%%%%%%%%% Error Catching Loop
catch
    ErrorMessage=lasterr;
    errordlg(ErrorMessage, 'Error Box')
    err=str2double(ErrorMessage);
end

%%%%%%%%%%%%%%%%%%%%%%%%%%%%%%%%%%%%% Check Box
if err==0
    app.CheckBoxEditField.Value='Process Accomplished!';
    app.Lamp.Color='g';
else
    app.CheckBoxEditField.Value='Check the Input Values!';
    app.Lamp.Color='red';
return
end
```

**Figure 47** Error Determination and End of 1<sup>st</sup> Run Button

### 6.3.2 Lower Body Correlation Implementation

Coding at the lower body, start by taken the data out of upper body. Such as

```
try
err=0;

syms x y z

g=9.81; % gravity (m/s^2)
app.Tliq=app.Tliq+273.15; %% liquid Temp from previous call back
%x1=0.3;
length=app.DistributorTubeLengthmmEditField.Value*(10^-3); %Distributor Length in m
capacity=app.EvaporatorCapacitykWEeditField.Value*(10^3); %Evaporator Capacity Input in W (j/s)
capacity_ton=capacity*0.28434516375*10^-3;
n_circuits=app.NumberofCircuitsEditField.Value; % Number of Circuits
```

**Figure 48** 2<sup>nd</sup> Run Button Input Reading

Nozzle Orifice Number Determination Loop followed the process above. The sample below represents small sample of determination code.

```
%%%%%%%%%%%%%% Nozzle Orifice Number & Nozzle Innder Diameter %
n_n=1; % n_n represents Nozzle Number- this one is created to read table B
if (strcmp(app.NozzleOrificeNumberDropDown.Value, '1/9 (0.90)'))
    n_n=n_n; %#ok<*ASGSL>
    dia_n=0.90*(10^-3);
elseif (strcmp(app.NozzleOrificeNumberDropDown.Value, '1/6 (1.10)'))
    n_n=n_n+1;
    dia_n=1.10*(10^-3);
elseif (strcmp(app.NozzleOrificeNumberDropDown.Value, '1/4 (1.40)'))
    n_n=n_n+2;
    dia_n=1.40*(10^-3);
elseif (strcmp(app.NozzleOrificeNumberDropDown.Value, '1/3 (1.60)'))
    n_n=n_n+3;
    dia_n=1.60*(10^-3);
elseif (strcmp(app.NozzleOrificeNumberDropDown.Value, '1/2 (1.80)'))
    n_n=n_n+4;
    dia_n=1.80*(10^-3);
elseif (strcmp(app.NozzleOrificeNumberDropDown.Value, '3/4 (2.20)'))
    n_n=n_n+5;
    dia_n=2.20*(10^-3);
elseif (strcmp(app.NozzleOrificeNumberDropDown.Value, '1 (2.60)'))
    n_n=n_n+6;
    dia_n=2.60*(10^-3);
.
.
.
```

**Figure 49** Nozzle Orifice Number Reading Loop

Next loop is generated to read pipe size.

```
%%%%%%%%%%%%%% Inlet Pipe Size Loop %%%%%%%%%%%%%%
if (strcmp(app.InletPipeDiametermmDropDown.Value, '12'))
    t_pipe=0.5;
    dia_p=(12-t_pipe)*(10^-3);
elseif (strcmp(app.InletPipeDiametermmDropDown.Value, '16'))
    t_pipe=0.5;
    dia_p=(16-t_pipe)*(10^-3);
elseif (strcmp(app.InletPipeDiametermmDropDown.Value, '19'))
    t_pipe=0.5;
    dia_p=(19-t_pipe)*(10^-3);
elseif (strcmp(app.InletPipeDiametermmDropDown.Value, '22'))
    t_pipe=0.5;
    dia_p=(22-t_pipe)*(10^-3);
elseif (strcmp(app.InletPipeDiametermmDropDown.Value, '28'))
    t_pipe=0.5;
    dia_p=(28-t_pipe)*(10^-3);
elseif (strcmp(app.InletPipeDiametermmDropDown.Value, '35'))
    t_pipe=1;
    dia_p=(35-t_pipe)*(10^-3);
elseif (strcmp(app.InletPipeDiametermmDropDown.Value, '42'))
    t_pipe=1;
    dia_p=(42-t_pipe)*(10^-3);
end
```

**Figure 50** Pipe Size Reading Loop

After conducting the determination loop, liquid and gas density, area and mass flux are found.

```
%%%%%%%%%%%%%% Necessary Eq.s %%%%%%%%%%%%%%
rho_lo=py.CoolProp.CoolProp.PropsSI('D', 'T',app.Tevap_i, 'Q', 0, app.ref);
rho_go=py.CoolProp.CoolProp.PropsSI('D', 'T',app.Tevap_i, 'Q', 1, app.ref);
rho_li=py.CoolProp.CoolProp.PropsSI('D', 'T',app.Tliq, 'Q', 0, app.ref);
rho_gi=py.CoolProp.CoolProp.PropsSI('D', 'T',app.Tliq, 'Q', 1, app.ref);
if (strcmp(app.RefrigerantSelectionDropDown.Value, 'R410A'))
V_l=py.CoolProp.CoolProp.PropsSI('V', 'T',app.Tevap_i, 'Q',0,'R410A');
else
V_l=py.CoolProp.CoolProp.PropsSI('V', 'T',app.Tevap_i, 'Q', 0, app.ref);
end
V_g=py.CoolProp.CoolProp.PropsSI('V', 'T',app.Tevap_i, 'Q', 1, app.ref);

%%%%%%%%% Calculations %%%%%%%%%%%%%%
A_p=3.1415*(dia_p^2)/4; % Pipe Area
A_t=3.1415*((app.dia_t)^2)/4; % Tube Area
del_h=app.h3-app.h2;
md=(capacity)/del_h; % mdot kg/s

%%%%%%%%% Re, G calculations %%%%%%%%%%%%%%
G_p=md/A_p; % Total Mass Flux at Pipe
%G_t=(md/A_t)/n_circuits; % Total Mass Flux at Tube
G_t=md/A_t;
```

**Figure 51** Necessary Equations, Area and Mass Flux Calculation

Void calculations take place

```
%Void Out
if (strcmp(app.RefrigerantSelectionDropDown.Value, 'R449 A'))
    sigma_o=6.59*10^-3; %% https://www.fridgespareswholesale.ie/sites/www.fridgespareswholesale.ie/files/r449a_technical_data_sheet.pdf
elseif (strcmp(app.RefrigerantSelectionDropDown.Value, 'R404A'))
    ref_up='R404A';
sigma_o=py.CoolProp.CoolProp.PropsSI('surface_tension', 'T',app.Tevap_i, 'Q',0,ref_up);
elseif (strcmp(app.RefrigerantSelectionDropDown.Value, 'R407C'))
    ref_up='R407C';
sigma_o=py.CoolProp.CoolProp.PropsSI('surface_tension', 'T',app.Tevap_i, 'Q',0,ref_up);
elseif (strcmp(app.RefrigerantSelectionDropDown.Value, 'R410A'))
    ref_up='R410A';
sigma_o=py.CoolProp.CoolProp.PropsSI('surface_tension', 'T',app.Tevap_i, 'Q',0,ref_up);
elseif (strcmp(app.RefrigerantSelectionDropDown.Value, 'R422D'))
    sigma_o=0.014;
elseif (strcmp(app.RefrigerantSelectionDropDown.Value, 'R422A'))
    sigma_o=0.013;
elseif (strcmp(app.RefrigerantSelectionDropDown.Value, 'R507'))
    ref_up='R507A';
sigma_o=py.CoolProp.CoolProp.PropsSI('surface_tension', 'T',app.Tevap_i, 'Q',0,ref_up);
else
sigma_o=py.CoolProp.CoolProp.PropsSI('surface_tension', 'T',app.Tevap_i, 'Q',0, app.ref); %surface tension (N/m)
end
void_o=(rho_lo*app.xn)/((rho_lo*app.xn)+rho_go*(1-app.xn));
Co=1+0.2*(1-app.xn)*(((9.81*app.dia_t)^0.25)*(rho_lo^0.5))/(G_t^0.5);
ugj_o=1.18*((9.81*sigma_o*(rho_lo-rho_go))^0.25)*(1-app.xn)/sqrt(rho_lo);
void_mix_o=((Co/void_o)+(rho_go*ugj_o/(app.xn*G_t)))^-1; % heterogeneous void fraction
```

**Figure 52** Void Calculations

Then, velocity, slip ratio, Pipe Reynolds Number and Tube Reynolds Number Calculations comes

```
%%%%%%%%%%%%%%%%%%%%%%%%%%%%%%%%%%%%%% u Velocity Calculations & Slip ratio %%%%%%%%%%%%%%%%%%%%%%%%%%%%%%%%%%
%Velocity in
u_gi=(md*app.xn)/(rho_gi*A_p*void_mix_i); % Velocity of gas "in"
u_li=(md*(1-app.xn))/(rho_li*A_p*(1-void_mix_i)); % Velocity of liquid "in"
s_i=u_gi/u_li; %% slip ratio "in"

%Velocity Out
u_g=((md*app.xn)/(rho_go*A_t*void_mix_o))/(n_circuits); %%void_mix_o); % Velocity of gas "out"
u_l=((md*(1-app.xn))/(rho_lo*A_t*(1-void_mix_o)))/(n_circuits); %%*(1-void_mix_o)); % Velocity of liquid "out"
s=u_g/u_l; %% slip ratio "out"
j_g=G_t*app.xn/rho_go; %gas superficial velo
j_l=G_t*(1-app.xn)/rho_lo; %liquid superficial velo
lambda=j_l/(j_l+j_g);
rhom=rho_lo*(1-void_mix_o)+rho_go*void_mix_o; %Heterogenous Density with respect to True Mean Velocity
rhom2=rho_lo*lambd+rho_go*(1-lambda) ;%written wrt superficial velocity
rhom3=((app.xn/rho_go)+(1-app.xn)/rho_lo)^-1; %rhom2=rhom3
V2=V_l*lambda+V_g*(1-lambda) ;%written wrt superficial velo

V_m=V_l*(1-void_mix_o)+V_g*void_mix_o;
%wm=md/(app.rho*A_t)/ n_circuits;

Re_p=G_p*dia_p./V_m; % Reynold's Number at Pipe
Re_t=(G_t*app.dia_t./V_m); %Reynold's Number at Tube
```

**Figure 53** Necessary Equations

Flow Pattern and Regime is evaluated by following:

```
%%%%%%%%%%%%%%%%%%%%%%%%%%%%%%%%%%%%%% REGIME MAP %%%%%%%%%%%%%%%%%%%%%%%%%%%%%%%%%%
G_l=(1-app.xn)*G_t;
G_g=app.xn*G_t;
%wl=wm*(1-app.xn); % liquid velocity at tube
%wg=wm*(app.xn); %gas velocity at tube
wl=((1-app.xn)/(1-void_mix_o))*md/(rho_lo*A_t)/n_circuits;
wg=(app.xn/void_mix_o)*md/(rho_go*A_t)/n_circuits;
wm=wl+wg;

Vd_l=wl/A_t;
Vd_g=wg/A_t;

%Re_l=wm*rho_lo*app.dia_t/V_l;
Re_l=G_l*app.dia_t/V_l;
Re_g=G_g*app.dia_t/V_g;
if Re_l>2000 %loop for liquid
    f_l=0.079/(Re_l^(1/4)); %Turbulent Flow
else
    f_l=16/Re_l; % Laminar Flow
end
if Re_g>2000 %loop for gas
    f_g=0.079/(Re_g^(1/4)); %Turbulent Flow
else
    f_g=16/Re_g; % Laminar Flow
end
delPz_l=(-2*f_l*(G_l^2)/(rho_lo*app.dia_t)); %% Cincolini eq.(25)
delPz_g=(-2*f_g*(G_g^2)/(rho_go*app.dia_t)); %% Cincolini eq.(25)
```

**Figure 54** Regime Map Primary Foundings

```

%X=((((1-app.xn)/app.xn)^0.875)*((rho_go/rho_lo)^0.5)*((V_1/V_g)^0.125)); %% Heat Atlas page 819 eq.(1) and/or Cioncolini
X=(delPz_1/delPz_g)^(1/2); %Cioncolini ex. (22)

%Inter to Bubbly
Y1_1=1.056*X^(-0.070);
Y1_2=-0.116*log(X)+1.283;

%Strat to Wavy
Y2_1=1.405*log(X)+7.521;
Y2_2=-1.337*log(X)+6.620;

%Wavy to Annular
Y3_1=0.813*X^(-0.077);
Y3_2=-0.214*log(X)+0.305;
Y3_3=0.412*X^(-1.188);
Y3_4=2.041*X^(-1.861);

```

**Figure 55** Regime Map Secondary Foundings

Regime Map Boundary curves which given between eq. (38) and eq. (46)

```

-----  

if 2<=X && X<=50 && 0.2<=Y1_1 && Y1_1<=1  

m=1;  

elseif 50<X && X<=9000 && 0.2<=Y1_2 && Y1_2<=0.8  

m=1;  

elseif 2<=X && X<=50 && 1<Y1_1  

m=5;  

elseif 50<X && X<=9000 && 0.8<Y1_2  

m=5;  

elseif 0.009<=X && X<=0.7 && 1<=Y2_1 && Y2_1<=6.9  

m=4;  

elseif 0.7<X && X<=70 && 1<=Y2_2 && Y2_2<=6.9  

m=4;  

elseif 0.009<=X && X<=0.7 && 6.9<=Y2_1 && Y2_1<=10^3  

m=3;  

... -- -- -- -- -

```

**Figure 56** Regime Map Boundary Codes

due to keeping report short I did not add further coding of map boundary

```

if m==1 %201
a1=13.98;
b1=-0.9501;
a2=0.1067;
b2=-0.2629;
c=3.577;
d=0.2029;
t=293;
elseif m==5 %200
a1=13.98;
b1=-0.9501;
a2=0.1067;
b2=-0.2629;
c=2.948;
d=0.2236;
t=304;
elseif m==4 %190
a1=13.98;
b1=-0.9501;
a2=0.0445;
b2=-0.1874;
c=9.275;
d=0.0324;
t=300;
elseif m==2

```

**Figure 57** Regime Map Friction Factor Codes

due to keeping report short I did not add further coding of friction factor codes

then pressure Drop for Nozzle, Momentum and Friction is written:

```
%%%%%% Nozzle Pressure Drop
wn=(md)/(app.rho*(3.1415*(dia_n^2)/4)); %Nozzle Velocity
b=dia_n/dia_p;
c_d=0.995;
cd_n=(1-b^4);
delPn=(cd_n*((wn/c_d)^2)*app.rho/2)*(10^-3); %Nozzle Pressure Drop
```

**Figure 58** Nozzle Pressure Drop Codes

```
%%%%%% 2 Phase Acceleration Pressure Drop %%%%%%
delPa(((u_g^2)*rho_go*void_mix_o)+((u_1^2)*app.rho*(1-void_mix_o)))*(10^-3);
```

**Figure 59** Acceleration Pressure Drop Codes

```
%%%% 2 Frictional Pressure Drop %%%%%%
% 1 Phase Pressure Drop
Re_lo=G_t*app.dia_t/V_l;
Re_go=G_t*app.dia_t/V_g;
f1_o=0.079/(Re_lo^0.25);
fg_o=0.079/(Re_go^0.25);

delP_l=4*fm*(length/app.dia_t)*(G_t^2)/(2*rho_lo);
%delP_l=4*f1_o*(length/app.dia_t)*(G_t^2)/(2*rho_lo)
delP_g=4*fg_o*(length/app.dia_t)*(G_t^2)/(2*rho_go);

Y=(delP_g/delP_l)^(1/2);

if 0<Y && Y<9.5
    if 1900<G_t
        B=55/(G_t^(1/2));
    elseif 500<G_t && G_t<1900
        B=2400/G_t;
    elseif G_t<=500
        B=4.8;
    end
elseif 9.5<Y && Y<28
    if G_t<=600
        B=520/(Y*G_t^(1/2));
    elseif 600<G_t
        B=21/Y;
    end
elseif 28<Y
    B=1500/((Y^2)*G_t^(1/2));
end
%%% Frictional Multiplier
G_t;
Y;
B;
n=0.25;
Q=1+((Y^2)-1)*(B*(app.xn^((2-n)/2))*((1-app.xn)^((2-n)/2))+app.xn^(2-n)); %Notice it is already squared
%%% 2 Phase Frictional Pressure Drop
delPf=delP_l*Q*(10^-3)/n_circuits;
```

**Figure 60** Frictional Pressure Drop Codes

By eliminating pressure drop, program completes its mission. By revising Sporlan catalog, we decided to add percent loading calculations for:

- R-134A
- R-401A
- R-409A
- R-22
- R-407C
- R-410A
- R-422D
- R-404A
- R-422A
- R-507

To eliminate this part, interpolation, data reading and value processing methods are followed. Due to having so much page so far, I would like to show sample places of percent loading evaluation part.

```

Tevap2=app.Tevap-273.15; %converted to read table
%Tevap2=app.Tevap_i;

syms x y z
data_A=readtable('TableA.xlsx');
k1=data_A(1:5,1);
k1=table2array(k1);
for i=1:5
    q=abs(Tevap2-k1(i,1));
    a1(i,:)=q; %#ok<*AGROW>
    i=i+1; %#ok<*FXSET>
end
b1=a1;
n = 2;
val = zeros(n,1);
for i=1:n
    [val(i),idx] = min(a1);
    a1(idx) = [];
end
[r1,c1]=find(b1==val(1));
[r2,c2]=find(b1==val(2));
r=[r1,c1;r2,c2];
m1=m1(:,id);

o1=[x;x;x]; %#ok<*NODEF>
if Tevap2<=4.44 && Tevap2>=-40
    o1(1,1)=m1(r1,1);
    o1(3,1)=m1(r2,1);
        if o1(1,1)<o1(3,1)
            o1([1 3],:)=o1([3 1],:);
        end
elseif Tevap2>4.44
    o1(2,1)=m1(r1,1);
    o1(3,1)=m1(r2,1);
        if o1(2,1)<o1(3,1)
            o1([2 3],:)=o1([3 2],:);
        end
elseif Tevap2<-40
    o1(1,1)=m1(r1,1);
    o1(2,1)=m1(r2,1);
        if o1(1,1)<o1(2,1)
            o1([1 2],:)=o1([2 1],:);
        end
end
B1=o1;
[A1,B1]; %#ok<*VUNUS>
A1_ans=((A1(2,1)-A1(1,1))/(A1(3,1)-A1(1,1)));
B1_ans=((B1(2,1)-B1(1,1))/(B1(3,1)-B1(1,1)));
eq=A1_ans=B1_ans;
x=solve(eq,x);
x=vpa(x);
x=round(x,5);
x=double(x);

```

**Figure 61** Percent Loading reading and Iteration

Overall, percent loading is obtained via reading Table A-8 and A-9 on the appendix and their conversion to metric system and integration to pressure drop software.

```

%%%%%%%%%%%%% Percentage Calculations %%%%%%
P_tube=((capacity_ton/n_circuits)/(x*y*z))*100;
P_nozzle=(capacity_ton/(p*z))*100;

%%%%%%%%%%%%%%%%%%%%%%%%%%%%%%%% Answer Bar %%%%%%
app.TubePkPaEditField_ans.Value=delPf+delPa;
app.NozzlePkPaEditField_ans.Value=delPn;
app.TotalPkPaEditField_ans.Value=delPa+delPf+delPn;
app.TubePercentLoadingEditField.Value=P_tube;
app.NozzlePercentLoadingEditField.Value=P_nozzle;

%%%%%%%%%%%%%%%%%%%%%%%%%%%%%%%% Error Finding Loop %%%%%%
catch
    ErrorMessage=lasterr;
    errordlg(ErrorMessage, 'Error Box')
    err=str2double(ErrorMessage);
end

%%%%%%%%%%%%%%%%%%%%%%%%%%%%%%%% Check Box Message %%%%%%
if err==0
app.CheckBoxEditField.Value='Process Accomplished!';
app.Lamp.Color='g';
else
app.CheckBoxEditField.Value='An Error Exist!';
app.Lamp.Color='red';
return
end

```

**Figure 62** Last Coding lines

By eliminating the above codes, coding comes to end by following lines

## 7. RESULT and DISCUSSION

In this section, comparisons of the developed software and existing software will be proceeded. Also, software output and experimental output will be discussed and accuracy of the software will be examined.

### 7.1 Existing Software and Developed Software Comparisons

To compare developed software output and existing software output, three different study is held in different time during coding process. 50 overall case is examined and their comparisons are made. Before proceeding to overall comparison data between existing software and developed one, let us examine some samples and see how outputs are given in both softwares.

let us examine Case 7.1.1

REFRIGERANT DISTRIBUTOR SELECTION DATA (Using NIST RefProp DLL)															
Refrigerant R- 404A(HP62)				Number of Circuits: 6											
Evaporator Temperature (°C): -5			Dist Tube Length (mm): 750												
Liquid Temperature (°C): 30			Evaporator Capacity (kW): 15,0												
Tube OD (in)	Tube ΔP (kPa)	Percent Loading	Nozzle Orifice Number	Nozzle ΔP (kPa)	Percent Loading	Total ΔP (kPa)									
1/4	63	94	4	252	133	315									

Figure 63 Case 7.1.1 Existing Software

Output Tree											
T (C) -5	x 0.2995	P (kPa) 516.8	Density (kg/m <sup>3</sup> ) 83.33	Enthalpy (kj/kg) 242.4	Cp (kj.K/kg) 5.824	Cv (kj.K/kg) 1.3	Pcrit (kPa) 3682	Psat (kPa) 516.8	Tcrit (C) 71.32	Tsat (C) -5.433	Viscosity (PA.s) 1.078e-05
Distributor Properties											
Nozzle Percent Loading % 129.3	Nozzle ΔP (kPa) 228.4	Tube Percent Loading % 90.78	Tube ΔP (kPa) 63.16	<input checked="" type="checkbox"/> Check Box <div style="border: 1px solid black; padding: 5px;">Process Accomplished!</div>							
Total ΔP (kPa) 291.5											MARMARA UNIVERSITESI
											FRITERM

Figure 64 Case 7.1.1 Developed Software

let us examine Case 7.1.2

REFRIGERANT DISTRIBUTOR SELECTION DATA (Using NIST RefProp DLL)													
Refrigerant R- 134a				Number of Circuits: 8									
Evaporator Temperature (°C): -5			Dist Tube Length (mm): 750										
Liquid Temperature (°C): 40			Evaporator Capacity (kW): 10,0										
Tube OD (in)	Tube ΔP (kPa)	Percent Loading	Nozzle Orifice Number	Nozzle ΔP (kPa)	Percent Loading	Total ΔP (kPa)							
1/4	29	56	4	166	144	195							

Figure 65 Case 7.1.2 Existing Software

Selection Tree	Refrigerant Tree	Distributor Tree									
Refrigerant Selection: R134A Tube ID (in): 1/4 Tube Wall Thickness (mm): 0.762	Superheating Difference (C): 0 Evaporator Temp. (C): -5 Subcooling Difference (C): 0 Condensation Temp. (C): 40  <b>RUN !</b>	Number of Circuits: 8 Distributor Tube Length (mm): 750 Nozzle Orifice Number: 4 (5.10) Inlet Pipe Diameter (mm): 22 Evaporator Capacity (kW): 10									
<b>RUN !</b>											
Output Tree											
T (C) -5	x 0.3118	P (kPa) 243.3	Density (kg/m³) 37.96	Enthalpy (kJ/kg) 256.4	Cp (kJ.K/kg) 1.936	Cv (kJ.K/kg) 1.166	Pcrit (kPa) 4059	Psat (kPa) 243.3	Tcrit (C) 101.1	Tsat (C) -5	Viscosity (PA.s) 1.032e-05
Distributor Properties											
Nozzle Percent Loading % 132.4	Nozzle ΔP (kPa) 163.9	Tube Percent Loading % 57.46	Tube ΔP (kPa) 41.84	Check Box <input checked="" type="checkbox"/> Process Accomplished!							
 MARMARA  FRITECH											

Figure 66 Case 7.1.2 Developed Software

let us examine Case 7.1.4

REFRIGERANT DISTRIBUTOR SELECTION DATA (Using NIST RefProp DLL)							
Refrigerant R- 1234yf				Number of Circuits: 6			
Evaporator Temperature (°C): 0		Dist Tube Length (mm): 500					
Liquid Temperature (°C): 30		Evaporator Capacity (kW): 15,0					
Tube OD (in)	Tube ΔP (kPa)	Percent Loading	Nozzle Orifice Number	Nozzle ΔP (kPa)	Percent Loading	Total ΔP (kPa)	
1/4	54	84	6	125	115	178	

Figure 67 Case 7.1.3 Existing Software

Selection Tree	Refrigerant Tree	Distributor Tree																								
Refrigerant Selection: R1234 yf Tube ID (in): 1/4 Tube Wall Thickness (mm): 0.762	Superheating Difference (C): 0 Evaporator Temp. (C): 0 Subcooling Difference (C): 0 Condensation Temp. (C): 30  <b>RUN !</b>	Number of Circuits: 6 Distributor Tube Length (mm): 500 Nozzle Orifice Number: 6 (6.20) Inlet Pipe Diameter (mm): 22 Evaporator Capacity (kW): 15																								
<b>RUN !</b>																										
<b>Output Tree</b> <table border="1"> <tr> <td>T (C)</td> <td>x</td> <td>P (kPa)</td> <td>Density (kg/m³)</td> <td>Enthalpy (kj/kg)</td> <td>Cp (kj.K/kg)</td> <td>Cv (kj.K/kg)</td> <td>Pcrit (kPa)</td> <td>Psat (kPa)</td> <td>Tcrit (C)</td> <td>Tsat (C)</td> <td>Viscosity (PA.s)</td> </tr> <tr> <td>0</td> <td>0.2481</td> <td>315.8</td> <td>68.03</td> <td>240.5</td> <td>1.709</td> <td>0.9159</td> <td>3382</td> <td>315.8</td> <td>94.7</td> <td>3.752e-5</td> <td>1.2e-05</td> </tr> </table>			T (C)	x	P (kPa)	Density (kg/m³)	Enthalpy (kj/kg)	Cp (kj.K/kg)	Cv (kj.K/kg)	Pcrit (kPa)	Psat (kPa)	Tcrit (C)	Tsat (C)	Viscosity (PA.s)	0	0.2481	315.8	68.03	240.5	1.709	0.9159	3382	315.8	94.7	3.752e-5	1.2e-05
T (C)	x	P (kPa)	Density (kg/m³)	Enthalpy (kj/kg)	Cp (kj.K/kg)	Cv (kj.K/kg)	Pcrit (kPa)	Psat (kPa)	Tcrit (C)	Tsat (C)	Viscosity (PA.s)															
0	0.2481	315.8	68.03	240.5	1.709	0.9159	3382	315.8	94.7	3.752e-5	1.2e-05															
<b>Distributor Properties</b> <table border="1"> <tr> <td>Nozzle Percent Loading %</td> <td>Nozzle ΔP (kPa)</td> <td>Tube Percent Loading %</td> <td>Tube ΔP (kPa)</td> </tr> <tr> <td>Inf</td> <td>120.7</td> <td>Inf</td> <td>49.95</td> </tr> <tr> <td colspan="4">Total ΔP (kPa)</td> </tr> <tr> <td colspan="4">170.7</td> </tr> </table>			Nozzle Percent Loading %	Nozzle ΔP (kPa)	Tube Percent Loading %	Tube ΔP (kPa)	Inf	120.7	Inf	49.95	Total ΔP (kPa)				170.7											
Nozzle Percent Loading %	Nozzle ΔP (kPa)	Tube Percent Loading %	Tube ΔP (kPa)																							
Inf	120.7	Inf	49.95																							
Total ΔP (kPa)																										
170.7																										
Check Box <input checked="" type="checkbox"/> Process Accomplished!																										
 MARMARA  FITERM																										

Figure 68 Case 7.1.3 Developed Software

let us examine Case 7.1.4

REFRIGERANT DISTRIBUTOR SELECTION DATA (Using NIST RefProp DLL)							
Refrigerant R- 22		Number of Circuits: 8					
Evaporator Temperature (°C): 5		Dist Tube Length (mm): 450					
Liquid Temperature (°C): 30		Evaporator Capacity (kW): 15,0					
Tube OD (in)	Tube ΔP (kPa)	Percent Loading	Nozzle Orifice Number	Nozzle ΔP (kPa)	Percent Loading	Total ΔP (kPa)	
3/16	59	90	5	71	54	130	

**Figure 69** Case 7.1.4 Existing Software

Selection Tree	Refrigerant Tree	Distributor Tree				
<input type="text" value="Refrigerant Selection R22"/> <input type="text" value="Tube ID (in) 3/16"/> <input type="text" value="Tube Wall Thickness (mm) 0.762"/>	<input type="text" value="Superheating Difference (C) 0"/> <input type="text" value="Evaporator Temp. (C) 5"/> <input type="text" value="Subcooling Difference (C) 0"/> <input type="text" value="Condensation Temp. (C) 30"/> <input type="button" value="RUN !"/>	<input type="text" value="Number of Circuits 8"/> <input type="text" value="Distributor Tube Length (mm) 450"/> <input type="text" value="Nozzle Orifice Number 5 (5.70)"/> <input type="text" value="Inlet Pipe Diameter (mm) 42"/> <input type="text" value="Evaporator Capacity (kW) 15"/>				
<input type="button" value="RUN !"/>						
Output Tree						
<input type="text" value="T (C) 5"/> <input type="text" value="x 0.1529"/> <input type="text" value="P (kPa) 584.1"/> <input type="text" value="Density (kg/m3) 146.3"/> <input type="text" value="Enthalpy (kj/kg) 236.6"/> <input type="text" value="Cp (kj.K/kg) 0.1367"/> <input type="text" value="Cv (kj.K/kg) 4.646"/> <input type="text" value="Pcrit (kPa) 4990"/> <input type="text" value="Psat (kPa) 584.1"/> <input type="text" value="Tcrit (C) 96.15"/> <input type="text" value="Tsat (C) 5"/> <input type="text" value="Viscosity (PA.s) 1.902e-05"/>						
Distributor Properties						<input checked="checked" type="checkbox"/> <input style="border: 1px solid black; padding: 5px; width: 150px; height: 30px;" type="text" value="Process Accomplished!"/>
<input type="text" value="Nozzle Percent Loading % 55.61"/> <input type="text" value="Nozzle ΔP (kPa) 74.1"/> <input type="text" value="Tube Percent Loading % 90.05"/> <input type="text" value="Tube ΔP (kPa) 53.27"/> <input type="text" value="Total ΔP (kPa) 127.4"/>						
						 

**Figure 70** Case 7.1.4 Developed Software

let us examine Case 7.1.5

REFRIGERANT DISTRIBUTOR SELECTION DATA (Using NIST RefProp DLL)													
Refrigerant R- 32				Number of Circuits: 8									
Evaporator Temperature (°C): 0			Dist Tube Length (mm): 450										
Liquid Temperature (°C): 30			Evaporator Capacity (kW): 15,0										
Tube OD (in)	Tube ΔP (kPa)	Percent Loading	Nozzle Orifice Number	Nozzle ΔP (kPa)	Percent Loading	Total ΔP (kPa)							
3/16	37	68	3	117	78	154							

Figure 71 Case 7.1.5 Existing Software

Selection Tree	Refrigerant Tree	Distributor Tree																														
<input style="width: 150px; height: 20px; border: 1px solid black; border-radius: 5px; padding: 2px; margin-bottom: 5px;" type="text" value="Refrigerant Selection"/> <input style="width: 150px; height: 20px; border: 1px solid black; border-radius: 5px; padding: 2px; margin-bottom: 5px;" type="text" value="R32"/> <input style="width: 150px; height: 20px; border: 1px solid black; border-radius: 5px; padding: 2px; margin-bottom: 5px;" type="text" value="Tube ID (in)"/> <input style="width: 150px; height: 20px; border: 1px solid black; border-radius: 5px; padding: 2px; margin-bottom: 5px;" type="text" value="3/16"/> <input style="width: 150px; height: 20px; border: 1px solid black; border-radius: 5px; padding: 2px; margin-bottom: 5px;" type="text" value="Tube Wall Thickness (mm)"/>	<input style="width: 150px; height: 20px; border: 1px solid black; border-radius: 5px; padding: 2px; margin-bottom: 5px;" type="text" value="Superheating Difference (C)"/> <input style="width: 150px; height: 20px; border: 1px solid black; border-radius: 5px; padding: 2px; margin-bottom: 5px;" type="text" value="0"/> <input style="width: 150px; height: 20px; border: 1px solid black; border-radius: 5px; padding: 2px; margin-bottom: 5px;" type="text" value="Evaporator Temp. (C)"/> <input style="width: 150px; height: 20px; border: 1px solid black; border-radius: 5px; padding: 2px; margin-bottom: 5px;" type="text" value="0"/> <input style="width: 150px; height: 20px; border: 1px solid black; border-radius: 5px; padding: 2px; margin-bottom: 5px;" type="text" value="Subcooling Difference (C)"/> <input style="width: 150px; height: 20px; border: 1px solid black; border-radius: 5px; padding: 2px; margin-bottom: 5px;" type="text" value="0"/> <input style="width: 150px; height: 20px; border: 1px solid black; border-radius: 5px; padding: 2px; margin-bottom: 5px;" type="text" value="Condensation Temp. (C)"/> <input style="width: 150px; height: 20px; border: 1px solid black; border-radius: 5px; padding: 2px; margin-bottom: 5px;" type="text" value="30"/>	<input style="width: 150px; height: 20px; border: 1px solid black; border-radius: 5px; padding: 2px; margin-bottom: 5px;" type="text" value="Number of Circuits"/> <input style="width: 150px; height: 20px; border: 1px solid black; border-radius: 5px; padding: 2px; margin-bottom: 5px;" type="text" value="8"/> <input style="width: 150px; height: 20px; border: 1px solid black; border-radius: 5px; padding: 2px; margin-bottom: 5px;" type="text" value="Distributor Tube Length (mm)"/> <input style="width: 150px; height: 20px; border: 1px solid black; border-radius: 5px; padding: 2px; margin-bottom: 5px;" type="text" value="450"/> <input style="width: 150px; height: 20px; border: 1px solid black; border-radius: 5px; padding: 2px; margin-bottom: 5px;" type="text" value="Nozzle Orifice Number"/> <input style="width: 150px; height: 20px; border: 1px solid black; border-radius: 5px; padding: 2px; margin-bottom: 5px;" type="text" value="3 (4.40)"/> <input style="width: 150px; height: 20px; border: 1px solid black; border-radius: 5px; padding: 2px; margin-bottom: 5px;" type="text" value="Inlet Pipe Diameter (mm)"/> <input style="width: 150px; height: 20px; border: 1px solid black; border-radius: 5px; padding: 2px; margin-bottom: 5px;" type="text" value="22"/> <input style="width: 150px; height: 20px; border: 1px solid black; border-radius: 5px; padding: 2px; margin-bottom: 5px;" type="text" value="Evaporator Capacity (kW)"/> <input style="width: 150px; height: 20px; border: 1px solid black; border-radius: 5px; padding: 2px; margin-bottom: 5px;" type="text" value="15"/>																														
<input type="button" value="RUN !"/>																																
<input type="button" value="RUN !"/>																																
<b>Output Tree</b> <table border="1" style="width: 100%; border-collapse: collapse;"> <tr> <td style="padding: 2px;">T (C)</td> <td style="padding: 2px;">X</td> <td style="padding: 2px;">P (kPa)</td> <td style="padding: 2px;">Density (kg/m3)</td> <td style="padding: 2px;">Enthalpy (kj/kg)</td> <td style="padding: 2px;">Cp (kj/K/kg)</td> <td style="padding: 2px;">Cv (kj.K/kg)</td> <td style="padding: 2px;">Pcrit (kPa)</td> <td style="padding: 2px;">Psat (kPa)</td> <td style="padding: 2px;">Tr crit (C)</td> <td style="padding: 2px;">Tsat (C)</td> <td style="padding: 2px;">Viscosity (PA.s)</td> </tr> <tr> <td style="padding: 2px;">0</td> <td style="padding: 2px;">0.1754</td> <td style="padding: 2px;">813.1</td> <td style="padding: 2px;">114.6</td> <td style="padding: 2px;">255.3</td> <td style="padding: 2px;">-0.03417</td> <td style="padding: 2px;">8.56</td> <td style="padding: 2px;">5782</td> <td style="padding: 2px;">813.1</td> <td style="padding: 2px;">78.11</td> <td style="padding: 2px;">4.547e-05</td> <td style="padding: 2px;"></td> </tr> </table>									T (C)	X	P (kPa)	Density (kg/m3)	Enthalpy (kj/kg)	Cp (kj/K/kg)	Cv (kj.K/kg)	Pcrit (kPa)	Psat (kPa)	Tr crit (C)	Tsat (C)	Viscosity (PA.s)	0	0.1754	813.1	114.6	255.3	-0.03417	8.56	5782	813.1	78.11	4.547e-05	
T (C)	X	P (kPa)	Density (kg/m3)	Enthalpy (kj/kg)	Cp (kj/K/kg)	Cv (kj.K/kg)	Pcrit (kPa)	Psat (kPa)	Tr crit (C)	Tsat (C)	Viscosity (PA.s)																					
0	0.1754	813.1	114.6	255.3	-0.03417	8.56	5782	813.1	78.11	4.547e-05																						
<b>Distributor Properties</b> <table border="1" style="width: 100%; border-collapse: collapse;"> <tr> <td style="padding: 2px;">Nozzle Percent Loading %</td> <td style="padding: 2px;">Nozzle ΔP (kPa)</td> <td style="padding: 2px;">Tube Percent Loading %</td> <td style="padding: 2px;">Tube ΔP (kPa)</td> </tr> <tr> <td style="padding: 2px;">Inf</td> <td style="padding: 2px;">117.1</td> <td style="padding: 2px;">Inf</td> <td style="padding: 2px;">35.95</td> </tr> <tr> <td colspan="4" style="text-align: center; padding: 2px;">Total ΔP (kPa)</td> </tr> <tr> <td colspan="4" style="text-align: center; padding: 2px;">153.1</td> </tr> </table>									Nozzle Percent Loading %	Nozzle ΔP (kPa)	Tube Percent Loading %	Tube ΔP (kPa)	Inf	117.1	Inf	35.95	Total ΔP (kPa)				153.1											
Nozzle Percent Loading %	Nozzle ΔP (kPa)	Tube Percent Loading %	Tube ΔP (kPa)																													
Inf	117.1	Inf	35.95																													
Total ΔP (kPa)																																
153.1																																
<div style="display: flex; align-items: center; justify-content: space-between;"> <span style="margin-right: 10px;">Check Box <input checked="" type="checkbox"/></span> <div style="border: 1px solid black; padding: 2px; width: fit-content;"> <span style="margin-right: 5px;">Process Accomplished!</span> </div> </div>																																

Figure 72 Case 7.1.5 Developed Software

To compare outputs of existing software and developed software, 5 different case is studied. In table 4 and 5, combined version of tube, nozzle and total pressure drop is given and their accuracy-error analysis are shown.

**Table 4** Comparison of Existing Software vs Developed Software

Case No	Case-1		Case-2		Case-3		Case-4		Case-5	
	Accuracy	Error	Accuracy	Error	Accuracy	Error	Accuracy	Error	Accuracy	Error
N	89.667	10.333	98.780	1.220	96.437	3.563	95.816	4.184	99.915	0.085
T	100.000	0.000	69.048	30.952	91.892	8.108	89.243	10.757	97.108	2.892
Total	91.901	8.099	94.660	5.340	95.107	4.893	97.935	2.065	99.386	0.614

**Table 5** Existing Software and Developed Software Output Accuracy Analysis

Case No	Case-1		Case-2		Case-3		Case-4		Case-5	
	Accuracy	Error	Accuracy	Error	Accuracy	Error	Accuracy	Error	Accuracy	Error
N	89.667	10.333	98.780	1.220	96.437	3.563	95.816	4.184	99.915	0.085
T	100.000	0.000	69.048	30.952	91.892	8.108	89.243	10.757	97.108	2.892
Total	91.901	8.099	94.660	5.340	95.107	4.893	97.935	2.065	99.386	0.614

## 7.2 Experimental Data and Developed Software Comparison

Developed software is tested under the investigation of Friterm A.S. Experiment process is explained under 5<sup>th</sup> title “EXPERIMENTEL SETUP AND VALIDATION”. In this section, experimental data and developed software data will be compared. Accuracy will be examined. Let's start with 1 Case. Scenario is given in Table 4

**Table 6** Experimental Case-7.2.1

Refrigerant	R-404A
Superheating Difference (°C)	6.5
Evaporator Temperature (°C)	0
Subcooling Difference (°C)	110
Condensation Temperature (°C)	40
Tube ID	1/4
Wall Thickness (mm)	0.68
Number of Circuits	5
Distributor Tube Length (mm)	1000
Nozzle Orifice Number	6
Evaporator Capacity (kW)	16.21
Nozzle Pressure Drop (kPa)	87.12
Tube Pressure Drop (kPa)	72.14
Total Pressure Drop	<b>159.26</b>

Selection Tree	Refrigerant Tree	Distributor Tree									
Refrigerant Selection: R404A	Superheating Difference (C) 6.5	Number of Circuits 5									
Tube ID (in) 1/4	Evaporator Temp. (C) 0	Distributor Tube Length (mm) 1000									
Tube Wall Thickness (mm) 0.68	Subcooling Difference (C) 10	Nozzle Orifice Number 6 (6.20)									
	Condensation Temp. (C) 40	Inlet Pipe Diameter (mm) 22									
	<b>RUN !</b>	Evaporator Capacity (kW) 16.21									
Output Tree											
T (C) 0	x 0.2643	P (kPa) 607.7	Density (kg/m3) 108.8	Enthalpy (kj/kg) 242.1	Cp (kj.K/kg) -4.37	Cv (kj.K/kg) 1.549	Pcrit (kPa) 3682	Psat (kPa) 607.7	Tcrit (C) 71.32	Tsat (C) -0.4256	Viscosity (P.a.s) 1.138e-05
Distributor Properties											
Nozzle Percent Loading % 72.21	Nozzle ΔP (kPa) 80.31	Tube Percent Loading % 94.03	Tube ΔP (kPa) 68.07	<input checked="" type="checkbox"/> Check Box <div style="border: 1px solid black; padding: 5px; width: fit-content;">Process Accomplished!</div>							
Total ΔP (kPa) 148.4											
 MARMARA  Friterm											

**Figure 73** Case 7.2.1 Developed Software Output

let us examine Case 7.2.2

**Table 7** Experimental Case-7.2.2

Refrigerant	R-404A
Superheating Difference (°C)	5.2
Evaporator Temperature (°C)	-8
Subcooling Difference (°C)	-10
Condensation Temperature (°C)	40
Tube ID	1/4
Wall Thickness (mm)	0.68
Number of Circuits	5
Distributor Tube Length (mm)	1000
Nozzle Orifice Number	6
Evaporator Capacity (kW)	13.086
Nozzle Pressure Drop (kPa)	91.77
Tube Pressure Drop (kPa)	72.2
Total Pressure Drop	<b>163.97</b>

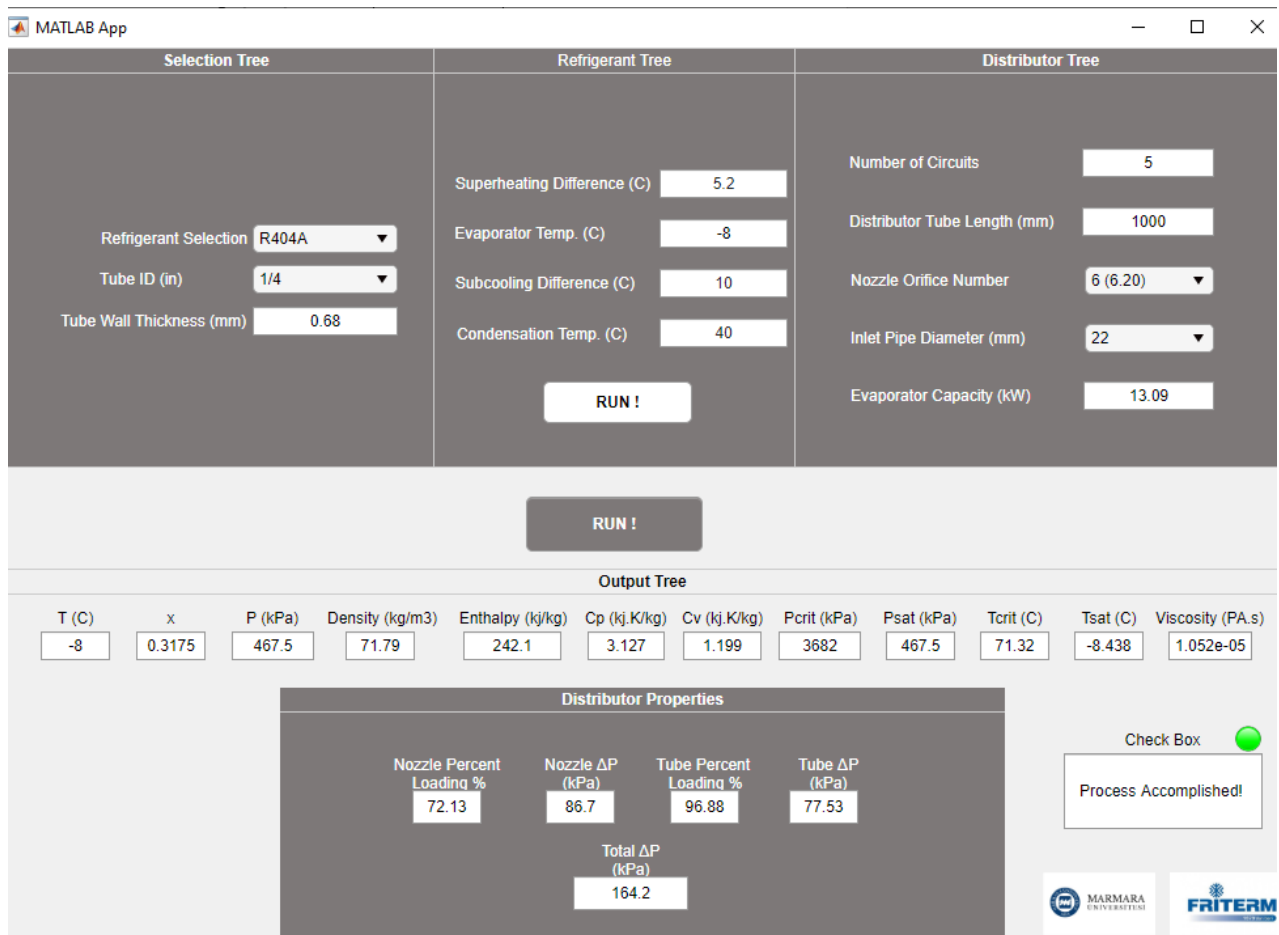


**Figure 74** Case-7.2.2 Developed Software Output

let us examine Case 7.2.3

**Table 8** Experimental Case-7.2.3

Refrigerant	R-404A
Superheating Difference (°C)	6.5
Evaporator Temperature (°C)	0
Subcooling Difference (°C)	10
Condensation Temperature (°C)	40
Tube ID	3/16
Wall Thickness (mm)	0.68
Number of Circuits	4
Distributor Tube Length (mm)	420
Nozzle Orifice Number	3
Evaporator Capacity (kW)	9.036
Nozzle Pressure Drop (kPa)	103.5
Tube Pressure Drop (kPa)	96.8
Total Pressure Drop	<b>200.3</b>

Selection Tree	Refrigerant Tree	Distributor Tree																																													
Refrigerant Selection R404A	Superheating Difference (C) 6.5	Number of Circuits 4																																													
Tube ID (in) 3/16	Evaporator Temp. (C) 0	Distributor Tube Length (mm) 420																																													
Tube Wall Thickness (mm) 0.68	Subcooling Difference (C) 10	Nozzle Orifice Number 3 (4.40)																																													
	Condensation Temp. (C) 40	Inlet Pipe Diameter (mm) 22																																													
	<b>RUN !</b>	Evaporator Capacity (kW) 9.036																																													
T (C) 0	X 0.2643	P (kPa) 607.7	Density (kg/m3) 108.8	Enthalpy (kj/kg) 242.1	Cp (kj.K/kg) -4.37	Cv (kj.K/kg) 1.549	Pcrit (kPa) 3682	Psat (kPa) 607.7	Tcrit (C) 71.32	Tsat (C) -0.4256	Viscosity (PA.s) 1.138e-05																																				
<table border="1"> <thead> <tr> <th colspan="12">Distributor Properties</th> </tr> </thead> <tbody> <tr> <td>Nozzle Percent Loading % 79.7</td> <td>Nozzle ΔP (kPa) 98.89</td> <td>Tube Percent Loading % 145.1</td> <td>Tube ΔP (kPa) 81.19</td> <td colspan="8"> <input checked="" type="checkbox"/> Check Box            Process Accomplished!         </td> </tr> <tr> <td colspan="12" style="text-align: center;">Total ΔP (kPa) 180.1</td> </tr> </tbody> </table>												Distributor Properties												Nozzle Percent Loading % 79.7	Nozzle ΔP (kPa) 98.89	Tube Percent Loading % 145.1	Tube ΔP (kPa) 81.19	<input checked="" type="checkbox"/> Check Box Process Accomplished!								Total ΔP (kPa) 180.1											
Distributor Properties																																															
Nozzle Percent Loading % 79.7	Nozzle ΔP (kPa) 98.89	Tube Percent Loading % 145.1	Tube ΔP (kPa) 81.19	<input checked="" type="checkbox"/> Check Box Process Accomplished!																																											
Total ΔP (kPa) 180.1																																															

**Figure 75** Case-7.2.3 Developed Software Output

let us examine Case-7.2.4

**Table 9** Experimental Case-7.2.4

Refrigerant	R-404A
Superheating Difference (°C)	5.2
Evaporator Temperature (°C)	-8
Subcooling Difference (°C)	10
Condensation Temperature (°C)	40
Tube ID	3/16
Wall Thickness (mm)	0.68
Number of Circuits	4
Distributor Tube Length (mm)	420
Nozzle Orifice Number	3
Evaporator Capacity (kW)	7.28
Nozzle Pressure Drop (kPa)	99
Tube Pressure Drop (kPa)	100
Total Pressure Drop	<b>199</b>

Selection Tree	Refrigerant Tree	Distributor Tree									
Refrigerant Selection: R404A Tube ID (in): 3/16 Tube Wall Thickness (mm): 0.68	Superheating Difference (C): 5.2 Evaporator Temp. (C): -8 Subcooling Difference (C): 10 Condensation Temp. (C): 40  <b>RUN !</b>	Number of Circuits: 4 Distributor Tube Length (mm): 420 Nozzle Orifice Number: 3 (4.40) Inlet Pipe Diameter (mm): 22 Evaporator Capacity (kW): 7.28									
<b>RUN !</b>											
Output Tree											
T (C)	x	P (kPa)	Density (kg/m3)	Enthalpy (kj/kg)	Cp (kj.K/kg)	Cv (kj.K/kg)	Pcrit (kPa)	Psat (kPa)	Tcrit (C)	Tsat (C)	Viscosity (PA.s)
-8	0.3175	467.5	71.79	242.1	3.127	1.199	3682	467.5	71.32	-8.438	1.052e-05
Distributor Properties											
Nozzle Percent Loading %	79.42	Nozzle ΔP (kPa)	106.3	Tube Percent Loading %	146.1	Tube ΔP (kPa)	92.39	Check Box <input checked="" type="checkbox"/> Process Accomplished!			
Total ΔP (kPa) 198.7											
 MARMARA UNIVERSITASI  FRITERM											

**Figure 76** Case-7.2.4 Developed Software Output

let us examine Case 7.2.5

**Table 10** Experimental Case-7.2.5

Refrigerant	R-404A
Superheating Difference (°C)	6.5
Evaporator Temperature (°C)	0
Subcooling Difference (°C)	10
Condensation Temperature (°C)	40
Tube ID	3/16
Wall Thickness (mm)	1
Number of Circuits	4
Distributor Tube Length (mm)	420
Nozzle Orifice Number	3
Evaporator Capacity (kW)	8.86
Nozzle Pressure Drop (kPa)	115
Tube Pressure Drop (kPa)	197
Total Pressure Drop	<b>312</b>

Refrigerant Selection R404A	Superheating Difference (C) 6.5	Number of Circuits 4																																													
Tube ID (in) 3/16	Evaporator Temp. (C) 0	Distributor Tube Length (mm) 420																																													
Tube Wall Thickness (mm) 1	Subcooling Difference (C) 10	Nozzle Orifice Number 3 (4.40)																																													
	Condensation Temp. (C) 40	Inlet Pipe Diameter (mm) 22																																													
	<b>RUN !</b>	Evaporator Capacity (kW) 8.86																																													
T (C) 0	x 0.2643	P (kPa) 607.7	Density (kg/m3) 108.8	Enthalpy (kj/kg) 242.1	Cp (kj.K/kg) -4.37	Cv (kj.K/kg) 1.549	Pcrit (kPa) 3682	Psat (kPa) 607.7	Tcrit (C) 71.32	Tsat (C) -0.4256	Viscosity (PA.s) 1.138e-05																																				
<table border="1"> <thead> <tr> <th colspan="12">Distributor Properties</th> </tr> </thead> <tbody> <tr> <td>Nozzle Percent Loading % 78.15</td> <td>Nozzle ΔP (kPa) 95.07</td> <td>Tube Percent Loading % 142.3</td> <td>Tube ΔP (kPa) 191.4</td> <td colspan="8"> <input checked="" type="checkbox"/> Process Accomplished!           </td> </tr> <tr> <td colspan="12" style="text-align: center;">Total ΔP (kPa) 286.5</td> </tr> </tbody> </table>												Distributor Properties												Nozzle Percent Loading % 78.15	Nozzle ΔP (kPa) 95.07	Tube Percent Loading % 142.3	Tube ΔP (kPa) 191.4	<input checked="" type="checkbox"/> Process Accomplished!								Total ΔP (kPa) 286.5											
Distributor Properties																																															
Nozzle Percent Loading % 78.15	Nozzle ΔP (kPa) 95.07	Tube Percent Loading % 142.3	Tube ΔP (kPa) 191.4	<input checked="" type="checkbox"/> Process Accomplished!																																											
Total ΔP (kPa) 286.5																																															
 MARMARA UNIVERSITY  FRITE																																															

**Figure 77** Case-7.2.5 Developed Software Output

For experimental comparison, 5 different case is studied. In table below, combined version of tube, nozzle and total pressure drop is given.

**Table 11** Comparison of Experimental Data and Software Output

Case No	Case-7.2.1		Case-7.2.2		Case-7.2.3		Case-7.2.4		Case-7.2.5	
	Exp.	Software	Exp.	Software	Exp.	Software	Exp.	Software	Exp.	Software
Nozzle	87.12	80.3	91.77	86.7	103.5	98.89	99	106.3	115	95.07
Tube	72.14	68.07	72.2	77.53	96.8	81.19	100	92.39	197	191.4
Total	159.26	148.37	163.97	164.23	200.3	180.08	199	198.69	312	287.1

In table below, accuracy and miss percentages of comparison is given.

**Table 12** Experimental Data and Software Output Accuracy Analysis

Case No	Case-7.2.1		Case-7.2.2		Case-7.2.3		Case-7.2.4		Case-7.2.5	
	Accuracy	Error	Accuracy	Error	Accuracy	Error	Accuracy	Error	Accuracy	Error
N	91.507	8.493	94.152	5.848	95.338	4.662	93.133	6.867	79.833	20.167
T	94.021	5.979	93.125	6.875	80.773	19.227	91.763	8.237	97.074	2.926
Total	92.660	7.340	99.842	0.158	88.772	11.228	99.844	0.156	91.327	8.673

### **7.3 Discussion**

To validate developed software, double check is done. At first, outputs of existing software and developed software is compared. The results showed accurate but that does not mean software is developed accurately. While for some cases, nozzle pressure drop exceeded, for some it become lower than the software. For some refrigerants, a need of refrigerant coefficient assign is occurred and this assignment is done via considering data comparison.

Kind of similar situation also exists for tube pressure drop. There was no need to assign coefficient for tube but for some cases tube pressure drop exceeded that the value offered by existing software and sometimes it become lower. Since, data difference with the existing software and developed software does not mean the program is wrong, experimental validation method is followed.

Experimental validation mostly had less than 10% of error and sometime less than 2%. Both nozzle and tube pressure drop resulted accurately. The error and accuracy analysis are given in Table 12.

Validation is done by two separate methods. Accuracy between experiment outputs and software output proved that the study is satisfied and required software is developed. Two expand the study, experimentation process can be done with different refrigerants. So, we can observe how software reacts on different refrigerant in different circumstances. These circumstances could be very long or short tube, temperature and pressure around critical values, and high or low kW energy of system. In addition, due to having different characteristics for different refrigerants, each of them may require to have coefficient to determine their flow characteristics and pressure drop.

Determining the pressure drop model was also an issue to overcome. Different correlations are studied such as: Lockhart-Martinelli, Friedel, Chisholm and Dukler. Chisholm's correlation is decided and applied to the software. Also determining nozzle pressure drop was not an easy task to handle. While some studies report that coefficient of nozzle pressure drop can be taken as constant, some studies refer to having the ratio between nozzle inlet and the outlet.

Due to lack of having 2-phase pressure drop software paper in the literature, the study is also proceeded as guessing the sources of errors during coding. To demonstrate these problems, at the beginning velocity of the liquid and gas so much more than actually it is supposed to be. Since we cannot see the exact velocity from experiment papers, I needed to realize dividing the velocity to number of circuits. Same problem also happened in Reynold's number and solved with the same method.

Other problems were not having accurate pressure drop for both nozzle and tube. Since Chisholm or any other scientist did not mention to find overall pressure drop and divide by number of circuits, I followed dividing the mass flux to number of circuit and finding the pressure drop at one tube. Another idea that emerges to overcome inaccurate pressure drop was to sum up all the diameters conducted to evaporator and find overall pressure drop. This one is also did not work.

While some solutions of the problems were an easy task, some had unpredicted solutions and these problems are overcome by repeating the literature study by over and over again.

## **8. CONCLUSION & RECOMMENDATION**

This study is emerged of not having an accurate two-phase pressure drop software existence in the industry. During the study, two-phase flow in horizontal refrigeration system is examined. During development process, existing correlations and deciding the most suitable and accurate method is examined and Chisholm's two-phase pressure drop model is decided. Chisholm's model was accurate on our study due to having accurate mass flow rate and studying channels from 0.90 mm to 25 mm. In addition to Chisholm's study, friction factor determination loop is created and flow regime is taken into account. In addition to new approaches, existing software, did not have subcooling/superheating section. By developing the mentioned software in this paper, we also conduct this approach.

To sum up, in these thesis report, two-phase pressure drop methodology is studied and commercial software is developed. Hence a feasible study is handled and by preceding validation, we can say that an accurate pressure drop module is created.

Further recommendations can made about the developed software. Due to proceeding experiments with R-404A only, experimental data check can be diversified by applying experimentation process with different refrigerants. New experiments can be done for extremely low or high kW capacity and same methodology for temperature as well. By proceeding this method, we would understand whether there may need to be update or the software is ready to run commercial activities.

Studied project is also open for future work. By providing the software with both external and internal sources -such as C# based software and data base- process time can be evaluated and optimization tool can be applied to see the best suitable distributor for input cases.

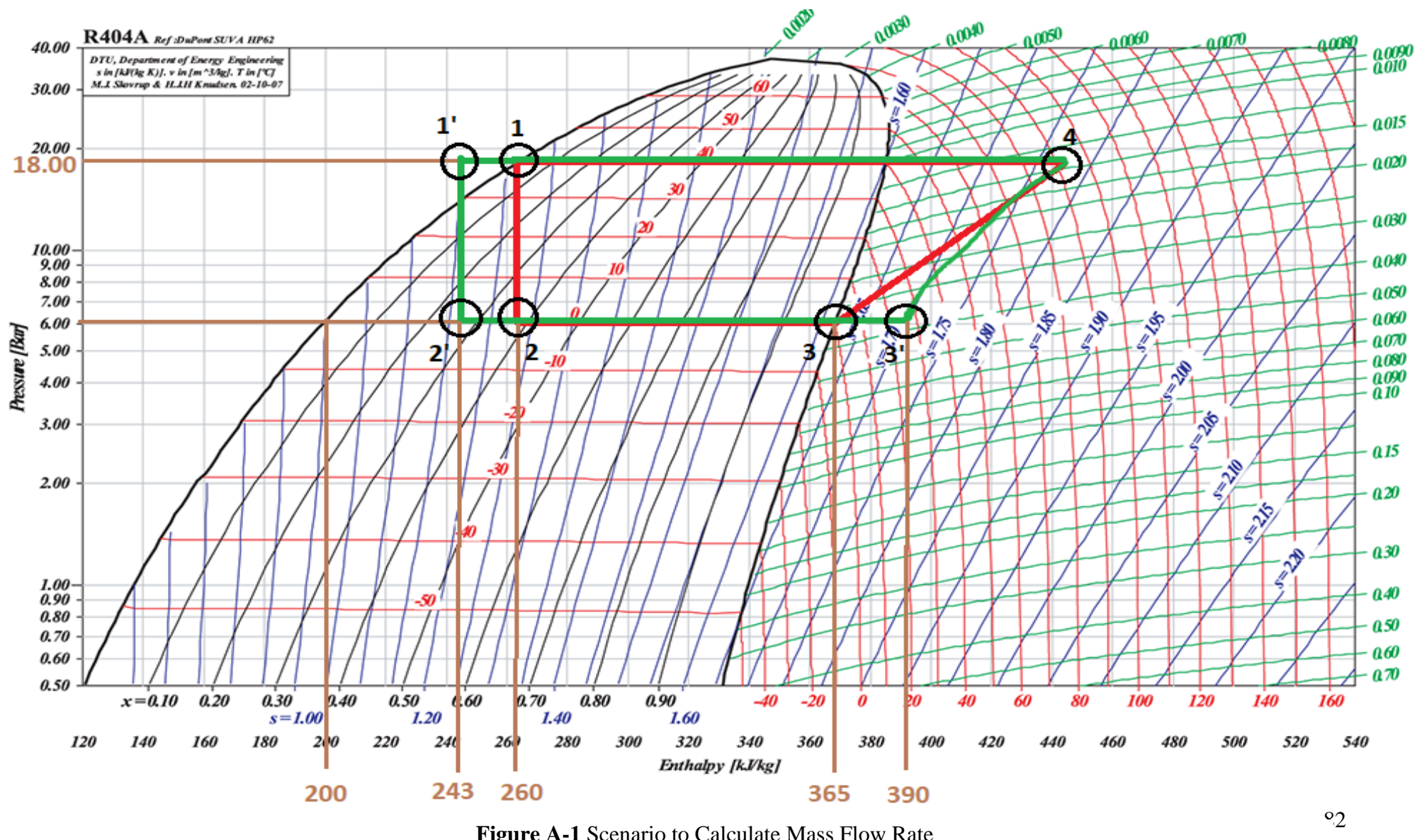
## 9. BIBLIOGRAPHY

- [1] “Cengel, Y. A., & Boles, M. A. (2007). Thermodynamics: An Engineering Approach 6th Editon (SI Units). The McGraw-Hill Companies, Inc., New”.
- [2] “J. H. Kim, J. E. Braun, and E. A. Groll, ‘Evaluation of a hybrid method for refrigerant flow balancing in multi-circuit evaporators,’ Int. J. Refrig., vol. 32, no. 6, pp. 1283–1292, 2009.”.
- [3] “F. Poggi, H. Macchi-Tejeda, A. Maréchal, D. Leducq, and A. Bontemps, ‘Experimental study of single and two-phase adiabatic flow distribution in compact heat exchangers,’ 18 th Fr. Congr. Mech. Eng., pp. 27–31, 2007.”.
- [4] “Cengel, Y. A., & Boles, M. A. (2007). Thermodynamics: An Engineering Approach 6th Editon (SI Units). The McGraw-Hill Companies, Inc., New York. Glossary Page:962”.
- [5] “Althouse, Andrew (2004). Modern Refrigeration and Air Conditioning. The Goodheart-Wilcox Company, Inc. p. 109. ISBN 1-59070-280-8.”.
- [6] “<https://thetech.com/vapour-compression-refrigeration-system/>”
- [7] “<https://www.superradiatorcoils.com/blog/4-main-refrigeration-cycle-components>”.
- [8] “<https://ph.parker.com/us/en/thermostatic-expansion-valve-parker-ebs-series/163525p>”.
- [10] “Sporlan-Parker February 2011 / BULLETIN 20-10”.
- [11] “Moreno Quiben, J. (2005). Experimental and analytical study of two-phase pressure drops during evaporation in horizontal tubes (No. THESIS). EPFL.”.
- [12] “Kind, M., Martin, H., Stephan, P., Roetzel, W., Spang, B., & Müller-Steinhagen, H. (2010). VDI Heat Atlas.”.
- [13] “Zuber N, Findlay JA (November 1965) Average volumetric concentration in two-phase flow systems. J Heat Transfer 87:453–468”.
- [14] “Kind, M., Martin, H., Stephan, P., Roetzel, W., Spang, B., & Müller-Steinhagen, H. (2010). VDI Heat Atlas. page 1121 L.2.1 Table 1”.
- [15] “Thome, J. R., & Cioncolini, A. (2016). Two-phase flow pattern maps for microchannels. In ENCYCLOPEDIA OF TWO-PHASE HEAT TRANSFER AND FLOW I: FUNDAMENTALS AND METHODS (pp. 47-84).”.

- [16] "J. Bandel. Druckverlust und Wärmeübergang bei der Verdampfung siedender Kältemittel im durchströmten waagerechten Rohr. PhD thesis, University of Karlsruhe, 1973.".
- [17] "D. R. H. Beattie and P. B. Whalley. A simple two-phase frictional pressure drop calculation method. *Int. J. Multiphase Flow*, 8:83–87, 1982.".
- [18] "K. Hashizume, H. Ogiwara, and H. Taniguchi. Flow pattern, void fraction and pressure drop of refrigerant two-phase flow in a horizontal pipe - II: Analysis of frictional pressure drop. *Int. J. Multiphase Flow*, 11:643–658, 1985.".
- [19] "R. W. Lockhart and R. C. Martinelli. Proposed correlation of data for isothermal two-phase, two-component in pipes. *Chem. Eng. Process*, 45(1):39–48, 1949.".
- [20] "S. G. Bankoff. A variable density single-fluid model two-phase flow with particular reference to steam-water. *J. Heat Transfer*, 11(Series B):265–272, 1960.".
- [21] "A. Cicchitti, C. Lombardi, M. Silvestri, and G. Soldaini R. Zavattarelli. Two-phase cooling experiments - pressure drop, heat transfer and burnout measurements. *Energia Nucleare*, 7(6):407–425, 1960.".
- [22] "J. R. S. Thom. Prediction of pressure drop during forced circulation boiling of water. *Int. J. Heat Mass Transfer*, 7:709–724, 1964.".
- [23] "B. Pierre. Flow resistance with boiling refrigerants - Part 1. *ASHRAE Journal*, 6(9):58–65, 1964.".
- [24] "C. J. Baroczy. A systematic correlation for two-phase pressure drop. *Chem. Eng. Prog. Symp. Ser.*, 62(44):232–249, 1965.".
- [25] "D. Chisholm. Pressure gradients due to friction during the flow of evaporating two-phase mixtures in smooth tubes and channels. *Int. J. Heat Mass Transfer*, 16:347–358, 1973.".
- [26] "L. Friedel. Improved friction drop correlations for horizontal and vertical two-phase pipe flow. In European Two-phase Flow Group Meeting, paper E2, Ispra, Italy, 1979.".
- [27] "H. Müller-Steinhagen and K. Heck. A simple friction pressure correlation for two-phase flow in pipes. *Chem. Eng. Process*, 20:297–308, 1986.".

- [28] "Thome, J. R., & Cioncolini, A. (2016). Two-Phase pressure drop. In ENCYCLOPEDIA OF TWO-PHASE HEAT TRANSFER AND FLOW I: FUNDAMENTALS AND METHODS (pp. 143-176).".

## 10. APPENDIX



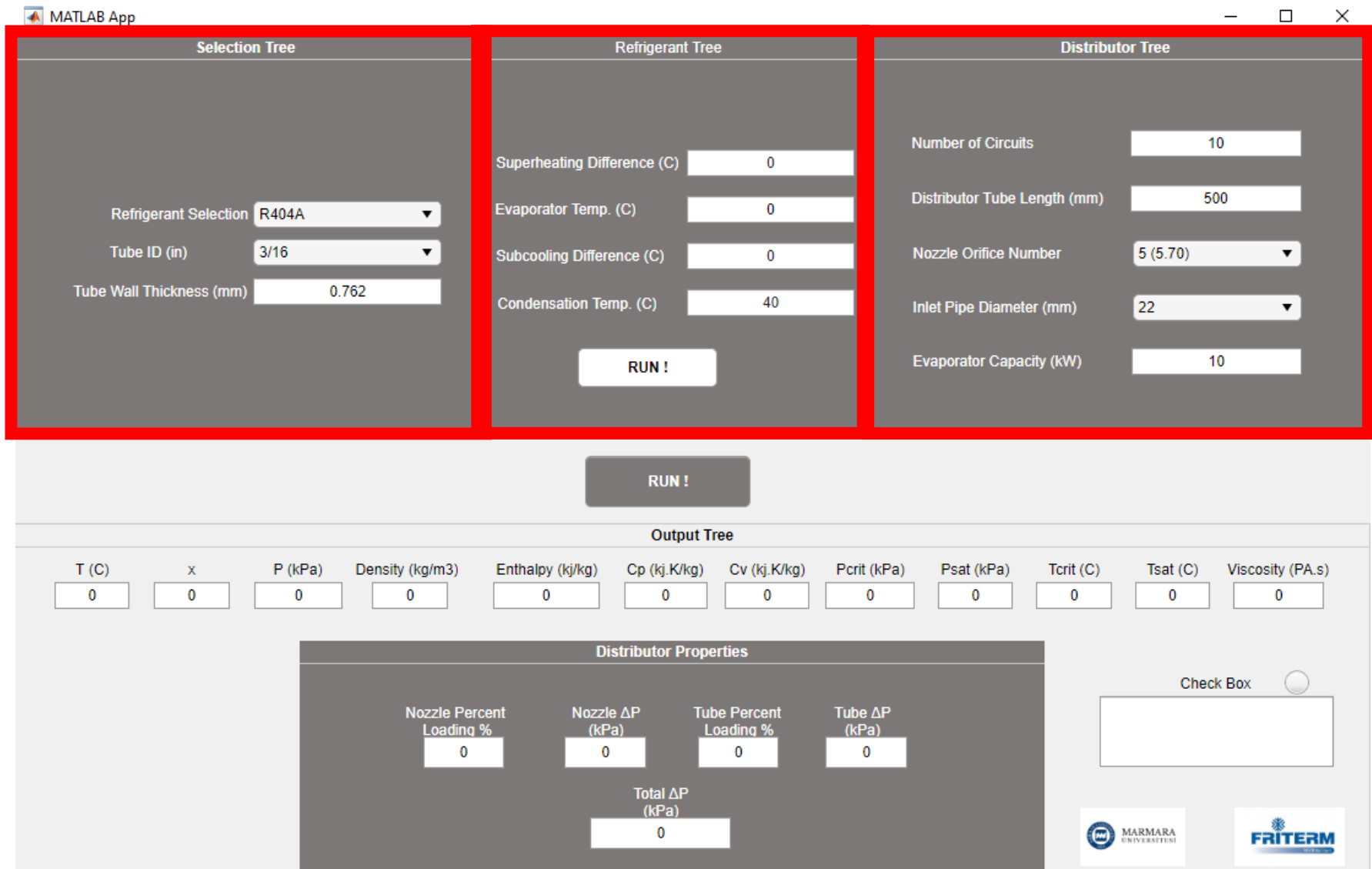


**Figure A-2** Default User Interface Red Squared Areas are Explained in the Further Pages

## Selection Tree

The image shows two separate selection panels, both titled "Selection Tree".

**Left Panel (Refrigerant Selection):**

- Refrigerant Selection dropdown: R404A (selected)
- Tube ID (in) dropdown: R134A, R22, R407C, R410A, R422D, R404A (selected), R422A, R507, R1234 yf, R1234 ze, R448 A, R449 A, R32, R717, R744.
- T (C) input field: 0
- X input field: 0

**Right Panel (Tube ID Selection):**

- Refrigerant Selection dropdown: R404A (selected)
- Tube ID (in) dropdown: 3/16 (selected)
- Tube Wall Thickness (mm) dropdown: 3/16, 1/4, 5/16, 3/8.

**Figure A-3** a) Refrigerant Selection Panel b) Tube ID Selection Panel

## Refrigerant Property Tree Section

The image shows a "Refrigerant Tree" panel with the following controls:

- Superheating Difference (C): 0
- Evaporator Temp. (C): 0
- Subcooling Difference (C): 0
- Condensation Temp. (C): 40
- RUN ! button

**Figure A-4** Refrigerant Temperature Tree

## Distributor Property Tree

**Distributor Tree**

Number of Circuits	10
Distributor Tube Length (mm)	500
Nozzle Orifice Number	5 (5.70) ▼
Inlet Pipe Diameter (mm)	22 ▼
Evaporator Capacity (kW)	10

**Figure A-5** Distributor Property Tree

T (C)	x	P (kPa)	Density (kg/m <sup>3</sup> )	Enthalpy (kj/kg)	Cp (kj.K/kg)	Cv (kj.K/kg)	Pcrit (kPa)	Psat (kPa)	Tcrit (C)	Tsat (C)	Viscosity (PA.s)
0	0	0	0	0	0	0	0	0	0	0	0

**Distributor Properties**

Nozzle Percent Loading %	Nozzle ΔP (kPa)	Tube Percent Loading %	Tube ΔP (kPa)
0	0	0	0
Total ΔP (kPa) 0			

Check Box

MARMARA UNIVERSITY  FRITERM 

**Figure A-6** Pressure Drop and Refrigerant Property Tree

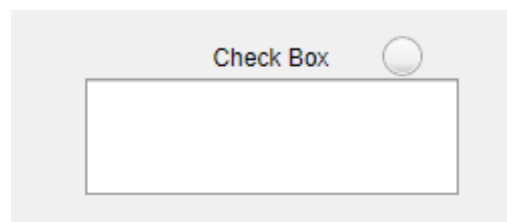


**Figure A-7** Check Box

Refrigerants 134a, 401A, 409A (4)

DISTRIBUTOR TUBE OD - Inches	REFRIGERANT											
	134a				401A				409A			
	EVAPORATOR TEMPERATURE (°F)											
	40°	20°	0°	-20°	40°	20°	0°	-20°	40°	20°	0°	-20°
3/16	0.30	0.21	0.16	0.12	0.33	0.26	0.20	0.16	0.27	0.20	0.16	0.12
1/4	0.85	0.62	0.47	0.36	0.96	0.73	0.57	0.46	0.77	0.58	0.45	0.36
5/16	1.73	1.26	0.95	0.73	1.94	1.48	1.16	0.93	1.57	1.19	0.92	0.72
3/8	3.12	2.27	1.70	1.31	3.47	2.65	2.07	1.65	2.84	2.14	1.65	1.30

Refrigerants 22 (5), 407C (5), 410A (7), 422D (5)

DISTRIBUTOR TUBE OD - Inches	REFRIGERANT											
	22				407C				410A			
	EVAPORATOR TEMPERATURE (°F)											
	40°	20°	0°	-20°	40°	20°	0°	-20°	40°	20°	0°	-20°
3/16	0.40	0.30	0.23	0.18	0.14	0.32	0.23	0.18	0.14	0.11	0.42	0.31
1/4	1.15	0.86	0.66	0.51	0.40	0.91	0.68	0.51	0.40	0.31	1.21	0.90
5/16	2.33	1.75	1.34	1.04	0.82	1.86	1.38	1.05	0.80	0.63	2.46	1.83
3/8	4.21	3.16	2.41	1.87	1.48	3.36	2.50	1.89	1.45	1.14	4.44	3.32
											2.51	1.91
											1.47	1.20
											2.60	1.89
											1.39	1.04
											0.79	0.73

Refrigerants 404A, 422A, 507 (5)

DISTRIBUTOR TUBE OD - Inches	REFRIGERANT											
	404A				422A				507			
	EVAPORATOR TEMPERATURE (°F)											
	40°	20°	0°	-20°	-40°	40°	20°	0°	-20°	-40°	40°	20°
3/16	0.28	0.21	0.15	0.12	0.09	0.23	0.17	0.12	0.09	0.07	0.28	0.20
1/4	0.81	0.59	0.44	0.33	0.26	0.67	0.49	0.36	0.26	0.20	0.81	0.59
5/16	1.66	1.21	0.90	0.68	0.52	1.37	0.98	0.73	0.54	0.40	1.65	1.21
3/8	2.99	2.18	1.62	1.22	0.94	2.48	1.79	1.31	0.97	0.72	2.99	2.18
											1.61	1.20
											0.91	

**Correction Factors for Other Distributor Tube Lengths**

TUBE LENGTH - Inches	12	18	24	30	36	42	48	54	60	66	72
CORRECTION FACTOR	1.36	1.16	1.07	1.00	0.95	0.90	0.86	0.82	0.79	0.76	0.73

**Correction Factors for Other Liquid Temperatures for Nozzle and Tubes (6)**

LIQUID TEMPERATURE °F	50°	60°	70°	80°	90°	100°	110°	120°
CORRECTION FACTOR	2.10	1.83	1.59	1.37	1.17	1.00	0.85	0.72

**Figure A-8 Refrigerant, Tube Length, Nozzle & Tube Correlations**

Refrigerants 22 (5), 407C (5), 410A (7), 422D (5)

DISTRIBUTOR NOZZLE NUMBER	REFRIGERANT											
	22				407C				410A			
	EVAPORATOR TEMPERATURE (°F)											
	40°	20°	0°	-20°	-40°	40°	20°	0°	-20°	-40°	40°	20°
1/9	0.14	0.11	0.09	0.07	0.06	0.11	0.08	0.07	0.06	0.05	0.16	0.13
1/6	0.21	0.16	0.13	0.11	0.09	0.17	0.13	0.10	0.09	0.07	0.25	0.20
1/4	0.34	0.26	0.21	0.18	0.15	0.27	0.21	0.17	0.14	0.12	0.40	0.31
1/3	0.44	0.34	0.28	0.23	0.20	0.35	0.27	0.22	0.18	0.15	0.53	0.41
1/2	0.61	0.48	0.38	0.32	0.27	0.48	0.38	0.30	0.25	0.21	0.73	0.57
3/4	0.92	0.72	0.58	0.48	0.41	0.72	0.57	0.46	0.38	0.32	1.10	0.86
1	1.23	0.96	0.78	0.64	0.55	0.97	0.76	0.61	0.50	0.43	1.47	1.15
1-1/2	1.79	1.40	1.13	0.94	0.80	1.41	1.10	0.89	0.73	0.62	2.14	1.67
2	2.46	1.92	1.55	1.29	1.10	1.94	1.51	1.22	1.00	0.88	2.93	2.30
2-1/2	3.06	2.39	1.93	1.60	1.37	2.41	1.88	1.52	1.25	1.06	3.66	2.86
3	3.68	2.87	2.32	1.92	1.65	2.90	2.26	1.82	1.50	1.28	4.39	3.44
4	4.92	3.84	3.10	2.58	2.20	3.88	3.03	2.43	2.01	1.71	5.88	4.60
5	6.07	4.74	3.82	3.18	2.72	4.78	3.73	3.00	2.48	2.11	7.25	5.67
6	7.28	5.68	4.58	3.81	3.26	5.73	4.48	3.60	2.98	2.52	8.69	6.80
8	8.77	6.84	5.52	4.59	3.92	6.91	5.39	4.34	3.58	3.05	10.5	8.19
10	9.83	7.67	6.19	5.14	4.40	7.74	6.05	4.86	4.02	3.42	11.7	9.18
12	12.1	9.47	7.64	6.35	5.43	9.56	7.47	6.00	4.96	4.22	14.5	11.3
15	15.0	11.7	9.48	7.88	6.73	11.9	9.26	7.45	6.15	5.23	18.0	14.1
17	16.8	13.1	10.6	8.81	7.53	13.3	10.4	8.33	6.88	5.85	20.1	15.7
20	20.3	15.8	12.8	10.6	9.08	16.0	12.5	10.0	8.29	7.05	24.2	19.0
25	25.5	19.9	16.1	13.4	11.4	20.1	15.7	12.6	10.4	8.87	30.5	23.8
30	29.1	22.7	18.4	15.3	13.0	23.0	17.9	14.4	11.9	10.1	34.8	27.2
35	35.1	27.4	22.1	18.4	15.7	27.6	21.6	17.3	14.3	12.2	41.9	32.8
40	39.3	30.7	24.8	20.6	17.6	31.0	24.2	19.5	16.1	13.7	47.0	36.7
50	51.0	39.8	32.1	26.7	22.8	40.2	31.4	25.2	20.9	17.7	60.9	47.7

**Figure A-9 Refrigerant & Nozzle Orifice Correlations**